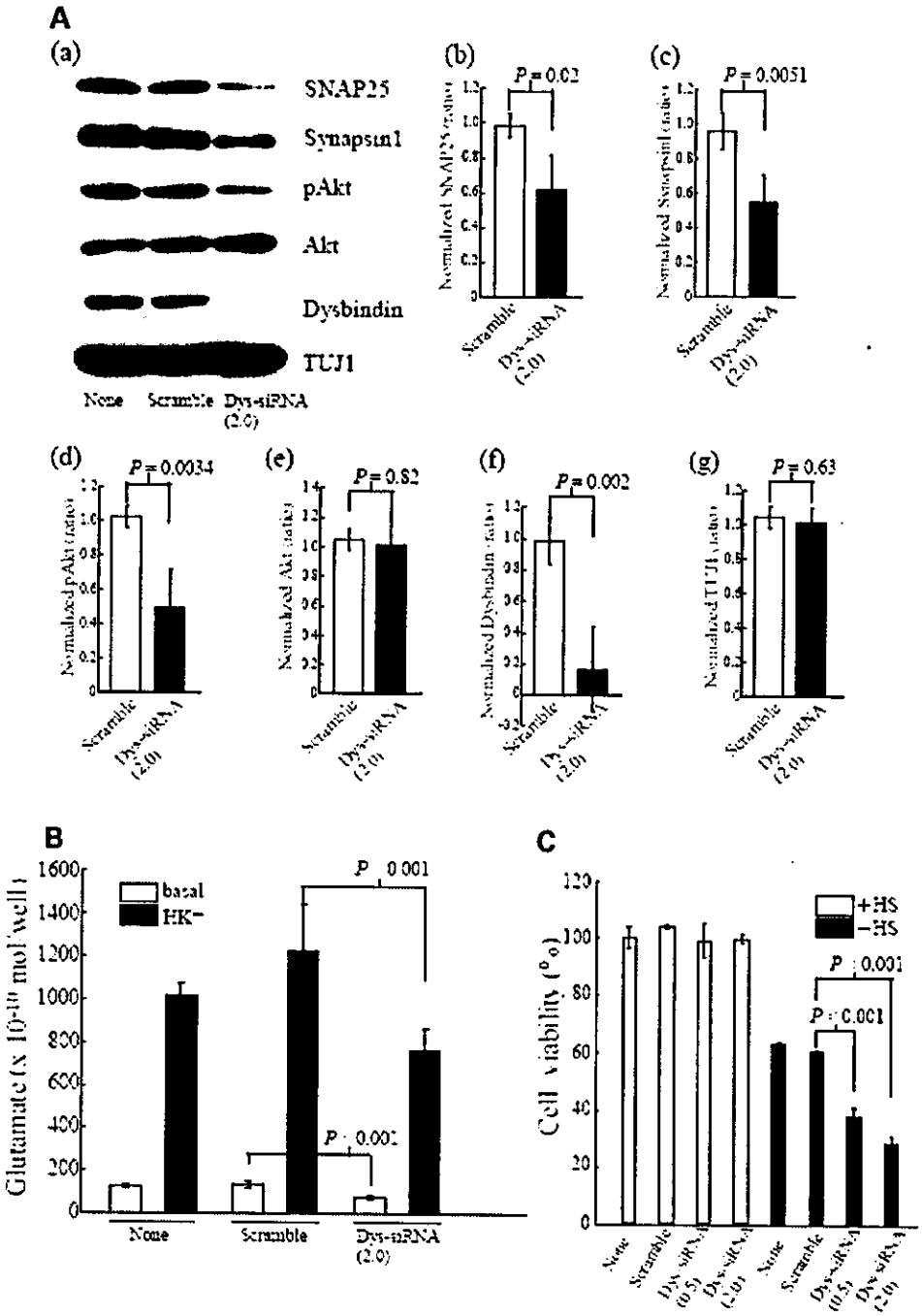

Figure 3. siRNA inhibition of endogenous dysbindin protein modulates protein expression, glutamate release and cell viability. (A) (a) Suppression of the pre-synaptic proteins and the phosphorylation of Akt in dysbindin-siRNA-transfected cultures. Cortical cultures after DIV4 were treated with siRNA for dysbindin (dys-siRNA; 2 mg/ml) or control (scramble; 2 mg/ml) for 72 h. Cortical cultures were harvested at DIV7 for western blotting for SNAP25, Synapsin I, pAkt, Akt, dysbindin or TUJ1. The immunoblots shown are representative of four independent experiments. (b–g) Quantification of the immunoreactivity of SNAP25, synapsin I, pAkt, total Akt, dysbindin and TUJ1. Data represent mean ± SD of the immunoreactivity from four independent experiments. (B) The reduced glutamate release in dysbindin-siRNA-transfected cultures. Cortical cultures were prepared without transfection (None), with transfection of control siRNA (Scramble; 2 mg/ml) or with transfection of siRNA for dysbindin (dys-siRNA; 2 mg/ml) at DIV4. Basal or HK^+ (50 mM KCl)-evoked release of glutamate was measured at DIV7 (after 72 h from transfection). Data represent the mean ± SD ($n = 6$). (C) Facilitation of neuronal death after serum deprivation by dysbindin-siRNA transfection. Cortical cultures after DIV4 were treated without transfection (None), with transfection of control siRNA (Scramble; 0.5 or 2 mg/ml) or with transfection of siRNA for dysbindin (dys-siRNA; 0.5 or 2 mg/ml) for 72 h. Deprivation of horse serum (HS) at DIV6 48 h after transfection is indicated as −HS. Cell viability was determined using the MTT assay at DIV7 72 h after the transfection and/or 24 h after HS deprivation. Data represent mean ± SD ($n = 8$).

the complex genetic diseases like schizophrenia (22). Alternatively, an unknown functional polymorphism, which is in LD with the SNPs and/or haplotypes, may be responsible for providing susceptibility to schizophrenia.

To date, association of dysbindin with schizophrenia has been confirmed across diverse populations. In addition, decreased expression of dysbindin mRNA and protein levels has been observed in prefrontal cortex and hippocampus of postmortem brain in schizophrenic patients (23–25). As dysbindin is distributed at least in part in axonal terminals (17), we focused on the possible role of dysbindin in neuronal transmission. We used two techniques, overexpression and knockdown, to investigate neuronal function of dysbindin. As the overexpression levels of dysbindin using sindbis virus were quite high when compared with the control level (~17-fold), the results could have non-physiological effects. However, the results from the knockdown experiments of the endogenous dysbindin protein were consistent with those from overexpression experiments. Our experiments suggest that dysbindin regulates the expression of SNAP25 and synapsin I proteins in the pre-synaptic machinery and is associated with increased glutamate release. SNAP25 is one of the fundamental molecular components of the SNARE (soluble *N*-ethylmaleimide-sensitive factor attachment protein receptors) protein complex, which is involved in intracellular vesicle trafficking and neurotransmitter release (18). Synapsin I is localized to the synaptic vesicles that are both docked and located away from the plasma membrane (18). Reduction of SNAP25 protein has been observed in frontal cortex of schizophrenia patients (26) and synapsin I protein was found to be reduced in the hippocampus of patients with schizophrenia (27). Hypofunction of glutamatergic system has been implicated in the neuropathology in schizophrenia (8). The abuse of phencyclidine, an NMDA receptor antagonist, results in positive symptoms, negative symptoms and cognitive impairments, similar to schizophrenic patients. The postmortem brain studies suggested impaired glutamatergic systems, e.g. reduced glutamate level, decreased AMPA receptor binding and expression and reduced NMDA receptor expression in several brain areas, including frontal cortex and hippocampus.

Our experiments also suggest the survival effect of dysbindin protein on cortical neurons against serum deprivation through the PI3-kinase-Akt signaling pathway. Thus, dysbindin might play an important role in neuronal vulnerability. Impaired PI3-kinase-Akt signaling in schizophrenia has been reported recently (28). Dysbindin expression in the brain of schizophrenic patients was reduced (23–25) and our data suggested that the downregulation of dysbindin expression suppressed the phosphorylation levels of Akt. Taken together, impaired PI3-kinase-Akt signaling in the schizophrenic brain might be due, in part, to the decreased expression of dysbindin. As dysbindin may affect neuronal viability through Akt activation, dysbindin-Akt signaling might be involved in early disruptions producing long-term vulnerability that leads to the onset of schizophrenia symptoms. As PI3-kinase-Akt signaling is activated by several growth factors such as brain-derived neurotrophic factor, nerve growth factor and insulin-like growth factors through tyrosine kinase receptors (19), the regulation of this system might be associated with dysbindin.

The Hermansky–Pudlak syndrome defines a group of autosomal recessive disorders characterized by deficiencies in lysosome-related organelles complex-1 (BLOC-1). Hermansky–Pudlak type-7 is caused by a nonsense mutation of dysbindin, which is a component of the BLOC-1 (29). Biological roles of BLOC-1 are still unknown; however, it might be involved in vesicle docking and fusion. Sandy mouse, which has a deleted dysbindin gene, expresses no dysbindin (29). Thus, this mouse could be a powerful tool for investigating brain function of dysbindin *in vivo*. It is of interest to examine the pre-synaptic protein expression, glutamate release, Akt phosphorylation and neuronal vulnerability *in vivo* using this mouse.

We have demonstrated the additional support for the genetic association between dysbindin and schizophrenia in a relatively large sample and the evidence of novel functions of dysbindin in cultured neurons. Our results suggest that an abnormality of dysbindin might influence glutamatergic systems and Akt signaling. Further investigation is necessary to elucidate the mechanisms of Akt activation and upregulation of pre-synaptic molecules by dysbindin.

MATERIALS AND METHODS

Subjects

Subjects for the association study were 670 patients with schizophrenia [males: 50.6%, mean age of 44.2 years (SD 14.6)] and 588 healthy comparison subjects [males: 48.7%, mean age of 36.2 years (SD 12.4)]. All the subjects were biologically unrelated Japanese patients. Consensus diagnosis was made for each patient by at least two psychiatrists according to the Diagnostic and Statistical Manual of Mental Disorders (DSM-IV) criteria. Control subjects were healthy volunteers who had no current or past contact to psychiatric services. After description of the study, written informed consent was obtained from every subject. The study protocol was approved by institutional ethical committees (Fujita Health University School of Medicine, Showa University School of Medicine and National Center of Neurology and Psychiatry).

SNP genotyping

Venous blood was drawn from the subjects and genomic DNA was extracted from whole blood according to the standard procedures. Six SNPs (P1655, P1635, P1325, P1320, P1763 and SNPA) adopted in the work of Straub *et al.* (2) and Williams *et al.* (21) were genotyped using the TaqMan 5′-exonuclease allelic discrimination assay, described previously (30,31). Briefly, the probes and primers for detection of the SNP were as follows. P1655: forward primer 5′-AGTTTTTAT CACTAATCAAAATGAAACAGCCTTT-3′, reverse primer 5′-CTCATTCTGTTATAACTAGTCTGACATGGT-3′, probe 1 5′-VIC-TATTAGCTATGATAGTGTTTTAT-MGB-3′ and probe 2 5′-FAM-ATTAGCTATGATAGTCTTTTAT-MGB -3′; P1635: forward primer 5′-GGAACTTTTCTTTGAAGA CTTCCTTTCG-3′, reverse primer 5′-ACCACTAACAACC AAAAAGAAAACAAACA-3′, probe 1 5′-VIC-TAAAGCC AATAATTACC-MGB-3′ and probe 2 5′-FAM-AGCCAG

TAATTACC-MGB-3′; P1325: forward primer 5′-GATATG ACTCCTTAATTCACAGGCTACAG-3′, reverse primer 5′-GTTACTGCACACAAGCAACTGTTAA-3′, probe 1 5′-VIC -AATGGATGTTGCATTAGT-MGB-3′ and probe 2 5′-FAM -ATGGATGTTGCGTTAGT-MGB-3′; P1320: forward primer 5′-CCAATCCATTCTTTTATTGACATGGAGTTT-3′, reverse primer 5′-TGATTTTGACCAAGTCCATTGTGTCT -3′, probe 1 5′-VIC-AAAAGCACAAACAACAAG-MGB-3′ and probe 2 5′-FAM-AAAAGCACAAATAACAAG-MGB-3′; P1763: forward primer 5′-GGCAGAAGCAGTGAGTGAGA-3′, reverse primer 5′-TGGGCTCTTATGTCTACCTTTCCTAAA -3′, probe 1 5′-VIC-TCACCTGGATGTCAGC-MGB-3′ and probe 2 5′-FAM-ACCTGGCTGTCAGC-MGB-3′; SNPA: forward primer 5′-TCTGTTATGTGCCATTCACTGTTTT-3′, reverse primer 5′-TAGGGCTGGGATTGGATGA-3′, probe 1 5′-VIC-AGCAGTTTACATCTGGG-MGB-3′ and probe 2 5′-FAM-AGCAGTTTACATCAGGG-MGB-3′. PCR cycling conditions were 95°C for 10 min, 45 cycles of 92°C for 15 s and 60°C for 1 min.

Cell culture

Dissociated cortical cultures were prepared from postnatal 2- or 3-day-old rat (SLC, Shizuoka, Japan) cortex, as described previously (32,33). Briefly, cells were gently dissociated with a plastic pipette after digestion with papain (90 U/ml, Sigma) at 37°C. The dissociated cells were plated at a final density of 5×10^5 per cm^2 on polyethyleneimine-coated 12- or 24-well plates (4 and 2 cm^2 surface area/well, respectively; Corning, NY, USA) or cover glasses (Matsunami, Osaka, Japan) attached to flexiperm (VIVASCIENCE, Gottingen, Germany). The culture medium consisted of 5% precolostrum newborn calf serum, 5% heated-inactivated horse serum and 90% of a 1 : 1 mixture of Dulbecco's modified Eagle's medium (DMEM) and Ham's F-12 medium containing 15 mM HEPES buffer, pH 7.4, 30 nM Na_2SeO_3 and 1.9 mg/ml of $NaHCO_3$.

Sindbis virus

A bicistronic vector plasmid (pSinEGdsp) was provided by Dr Kawamura (Niigata University, Japan). The plasmid was derived from pSinRep5 (Invitrogen, USA) and had two subgenomic promoters followed by a multiple cloning site for arbitrary gene insertion and an EGFP open reading frame, thus the virus can produce arbitrary protein and EGFP independently in the infected cell, as previously described (34). Dysbindin cDNAs amplified by RT–PCR with specific primer pairs (forward 5′-ACGCGTCAATGCTGGAGACCCTTCG-3′ and reverse 5′-GCATGCCAATTTAAGAGTCGCTGTCC-3′) were inserted at the *Mlu*I and *Sph*I sites of the plasmid. Each plasmid was cleaved with *Pac*I, and used as a template for mRNA transcription *in vitro* using mMESSAGE mMACHINE kit (Ambion, USA). Pseudovirions were produced according to the experimental procedure of Invitrogen. Baby hamster kidney (BHK) cells were transfected with each mRNA and 26S helper mRNA (Invitrogen) by electroporation (1250 V/cm, 50 μF, single pulse) using Gene Pulser2 (BioRad, USA). The cells were incubated with DMEM supplemented with 10% FCS for 24 h at 37°C, the supernatants were collected as pseudovirion-containing solutions.

Immunocytochemistry

Cultured neurons were fixed with 4% paraformaldehyde for 20 min and then rinsed three times with PBS. Subsequently, cultured cells were permeabilized with 0.2% Triton X-100 in PBS for 5 min at room temperature. The primary antibodies (anti-MAP2; Sigma) with 3% skim milk in PBS were applied overnight at 4°C. After washing, cells were incubated with secondary antibodies (Alexa Fluor, Molecular Probes) for 1 h at room temperature. Fluorescent images were captured by an inverted microscope (Axiovert 200, Zeiss) with a CCD (cool SNAPfx) purchased from Zeiss. Monochrome images were turned into color and analyzed using software (Slide BookTM 3.0, Intelligent Imaging Innovations, Inc., Denver, CO, USA). The images of GFP were analyzed with the same software.

Immunoblotting

Cells were lysed in SDS lysis buffer containing 1% SDS, 20 mM Tris–HCl (pH 7.4), 5 mM EDTA (pH 8.0), 10 mM NaF, 2 mM Na_3VO_4, 0.5 mM phenylarsine oxide and 1 mM phenylmethylsulfonyl fluoride. Lysates were centrifuged at 15 000 rpm for 60 min at 4°C, and the supernatants were collected for analysis. Samples were heat denatured with the standard SDS sample buffer. Immunoblottings were carried out as described previously (35). Briefly, immunoblottings were carried out with anti-SNAP25 antibody (1:3000, mouse monoclonal, Synaptic System, Gottingen, Germany), anti-synapsin I antibody (1:1000, rabbit anti-serum, Chemicon), anti-synaptotagmin antibody (1:1000, mouse monoclonal, BD Transduction Laboratory), anti-syntaxin antibody (1:3000, mouse monoclonal, Sigma), anti-GFP antibody (1:1000, rabbit polyclonal, MBL, Nagoya, Japan), anti-dysbindin antibody (23) (1:100, rabbit polyclonal), anti-TUJ1 antibody (1:5000, mouse monoclonal, Berkeley antibody company, CA, USA), anti-Akt antibody (1:1000, rabbit antiserum, Cell Signaling) and anti-phospho-Akt antibody (Ser473, 1:1000, rabbit anti-serum, Cell Signaling) in TBS containing 1% non-fat dried milk. The immunoblotting experiments were performed four times and they were quantitatively analyzed by capturing images on films using a scanner (Epson, Tokyo, Japan) in conjunction with the Lane and Spot Analyzer software (version 6.0, ATTO, Tokyo, Japan).

Anti-dysbindin antibody was produced as described previously (36). Briefly, the peptide synthesized (QSDEEEVQVD-TALC: 320–333 amino acid residue of human dysbindin, with no homology in any mammalian protein) was conjugated with maleimide-activated keyhole limpet hemocyanin and immunized to two rabbits. The titer was measured by ELISA and sera of high titer against the peptide were obtained from both rabbits. The sera were affinity purified by a column conjugated with the immunized peptide.

Detection of glutamate release

The amount of glutamate released from the cultures was measured as previously reported (33,35). The glutamate released into the modified HEPES-buffered Krebs–Ringer assay buffer (KRH; 130 mM NaCl, 5 mM KCl, 1.2 mM

NaH_2PO_4, 1.8 mM $CaCl_2$, 10 mM glucose, 1% bovine serum albumin and 25 mM HEPES, pH 7.4) were measured by HPLC (Shimadzu, Kyoto, Japan) with a fluorescence detector (excitation wavelength, 340 nm; emission wavelength, 445 nm, Shimadzu). For stimulation of cortical neurons, we used a HK^+ KRH solution consisting of 85 mM NaCl, 50 mM KCl, 1.2 mM NaH_2PO_4, 1.8 mM $CaCl_2$, 10 mM glucose, 1% bovine serum albumin and 25 mM HEPES, pH 7.4. Before exposing the cultures to HK^+ solution (1 min), basal fractions were collected. The glutamate release experiments were performed three times with independent cultures to confirm reproducibility.

MTT assay

To examine the cell viability, the metabolic activity of mitochondria was estimated by measuring the mitochondrial-dependent conversion of the 3-(4,5-dimethylthiazol-2-yl)-2,5-diphenyl tetrazolium bromide (MTT) (Sigma). We performed the viral infection or transfection of siRNA and then, the serum was deprived from culture medium. MTT (0.5 mg/ml in PBS) was added to each well at 24 h after serum deprivation. MTT was incubated for 1.5 h at 37°C. Then, the medium was carefully aspirated, and 200 µl of acidified isopropyl alcohol was added to solubilize the colored formazan product. Absorbance was determined at 550 nm on a scanning multi-well plate reader (Bio-Rad) after agitating the plates for 5 min on a shaker.

siRNA transfection

We used 23 nt siRNA duplexes with two 3′ overhanging nucleotides targeting position 182–204 (aagugacaagucaaga gaagcaa) of human dysbindin mRNA. Scrambled sequence (aacgaugagaacgaucaagaaga), which had no homology to any mammalian mRNA, was used as a control siRNA. Both sense and antisense strands were synthesized by Dharmacon Research Inc (Lafayette, PA, USA). SiRNA duplexes in the 2′-ACE deprotected and desalted form were dissolved in a 1× universal buffer (Dharmacon Research Inc). Transfection of both siRNAs was performed using NeuroPORTER™ (Gene Therapy Systems, Inc., San Diego, CA, USA), as reported (20).

Statistical analysis

Statistical analysis of association studies was performed using SNPAlyse (DYNACOM, Yokohama, Japan). The presence of Hardy–Weinberg equilibrium was examined by using the χ^2-test for goodness of fit. Allele distributions between patients and controls were analyzed by the χ^2-test for independence. The measure of LD, denoted as D', was calculated from the haplotype frequency using the expectation–maximization algorithm. Case–control haplotype analysis was performed by the permutation method to obtain the empirical significance (37). The global P-values represent the overall significance using the χ^2-test when the observed versus expected frequencies of all the haplotypes are considered together. The individual haplotypes were tested for association by grouping all others together and applying the χ^2-test with 1 df. P-values were calculated on the basis of 10 000 replications. Statistical analysis of neurobiological assays was performed by Students' t-test. All P-values reported are two tailed. Statistical significance was defined at $P < 0.05$. To be conservative, Bonferroni corrections were applied for multiple comparisons, e.g. number of analyzed SNPs and haplotypes, although SNPs were in LD.

ACKNOWLEDGEMENTS

We wish to thank Dr Meiko Kawamura for kindly providing a bicistronic vector plasmid, and Tomoko Shizuno and Reiko Fujita for technical assistance. This work was supported by Grants-in-Aid from the Japanese Ministry of Health, Labor and Welfare, the Japanese Ministry of Education, Culture, Sports, Science and Technology, the Uehara Memorial Foundation and Japan Foundation for Neuroscience and Mental Health.

REFERENCES

1. O'Donovan, M.C., Williams, N.M. and Owen, M.J. (2003) Recent advances in the genetics of schizophrenia. *Hum. Mol. Genet.*, **12**, R125–R133.
2. Straub, R.E., Jiang, Y., MacLean, C.J., Ma, Y., Webb, B.T., Myakishev, M.V., Harris-Kerr, C., Wormley, B., Sadek, H., Kadambi, B. *et al.* (2002) Genetic variation in the 6p22.3 gene *DTNBP1*, the human ortholog of the mouse dysbindin gene, is associated with schizophrenia. *Am. J. Hum. Genet.*, **71**, 337–348.
3. Schwab, S.G., Knapp, M., Mondabon, S., Hallmayer, J., Borrmann-Hassenbach, M., Albus, M., Lerer, B., Rietschel, M., Trixler, M., Maier, W. *et al.* (2003) Support for association of schizophrenia with genetic variation in the 6p22.3 gene, dysbindin, in sib-pair families with linkage and in an additional sample of triad families. *Am. J. Hum. Genet.*, **72**, 185–190.
4. Tang, J.X., Zhou, J., Fan, J.B., Li, X.W., Shi, Y.Y., Gu, N.F., Feng, G.Y., Xing, Y.L., Shi, J.G. and He, L. (2003) Family-based association study of DTNBP1 in 6p22.3 and schizophrenia. *Mol. Psychiatr.*, **8**, 717–718.
5. Van Den Bogaert, A., Schumacher, J., Schulze, T.G., Otte, A.C., Ohlraun, S., Kovalenko, S., Becker, T., Freudenberg, J., Jonsson, E.G., Mattila-Evenden, M. *et al.* (2003) The *DTNBP1* (dysbindin) gene contributes to schizophrenia, depending on family history of the disease. *Am. J. Hum. Genet.*, **73**, 1438–1443.
6. van den Oord, E.J., Sullivan, P.F., Jiang, Y., Walsh, D., O'Neill, F.A., Kendler, K.S. and Riley, B.P. (2003) Identification of a high-risk haplotype for the dystrobrevin binding protein 1 (*DTNBP1*) gene in the Irish study of high-density schizophrenia families. *Mol. Psychiatr.*, **8**, 499–510.
7. Morris, D.W., McGhee, K.A., Schwaiger, S., Scully, P., Quinn, J., Meagher, D., Waddington, J.L., Gill, M. and Corvin, A.P. (2003) No evidence for association of the dysbindin gene [*DTNBP1*] with schizophrenia in an Irish population-based study. *Schizophr. Res.*, **60**, 167–172.
8. Tsai, G. and Coyle, J.T. (2002) Glutamatergic mechanisms in schizophrenia. *Annu. Rev. Pharmacol. Toxicol.*, **42**, 165–179.
9. Weinberger, D.R., Egan, M.F., Bertolino, A., Callicott, J.H., Mattay, V.S., Lipska, B.K., Berman, K.F. and Goldberg, T.E. (2001) Prefrontal neurons and the genetics of schizophrenia. *Biol. Psychiatr.*, **50**, 825–844.
10. Moghaddam, B. (2003) Bringing order to the glutamate chaos in schizophrenia. *Neuron*, **40**, 881–884.
11. Harrison, P.J. and Owen, M.J. (2003) Genes for schizophrenia? Recent findings and their pathophysiological implications. *Lancet*, **361**, 417–419.
12. Buonanno, A. and Fischbach, G.D. (2001) Neuregulin and ErbB receptor signaling pathways in the nervous system. *Curr. Opin. Neurobiol.*, **11**, 287–296.
13. Stefansson, H., Sigurdsson, E., Steinthorsdottir, V., Bjornsdottir, S., Sigmundsson, T., Ghosh, S., Brynjolfsson, J., Gunnarsdottir, S.,

Ivarsson, O., Chou, T.T. *et al.* (2002) Neuregulin 1 and susceptibility to schizophrenia. *Am. J. Hum. Genet.*, **71**, 877–892.
14. Mothet, J.P., Parent, A.T., Wolosker, H., Brady, R.O., Jr, Linden, D.J., Ferris, C.D., Rogawski, M.A. and Snyder, S.H. (2000) D-serine is an endogenous ligand for the glycine site of the *N*-methyl-D-aspartate receptor. *Proc. Natl Acad. Sci. USA*, **97**, 4926–4931.
15. Chumakov, I., Blumenfeld, M., Guerassimenko, O., Cavarec, L., Palicio, M., Abderrahim, H., Bougueleret, L., Barry, C., Tanaka, H., La Rosa, P. *et al.* (2002) Genetic and physiological data implicating the new human gene G72 and the gene for D-amino acid oxidase in schizophrenia. *Proc. Natl Acad. Sci. USA*, **99**, 13675–13680.
16. De Blasi, A., Conn, P.J., Pin, J. and Nicoletti, F. (2001) Molecular determinants of metabotropic glutamate receptor signaling. *Trends Pharmacol. Sci.*, **22**, 114–120.
17. Benson, M.A., Newey, S.E., Martin-Rendon, E., Hawkes, R. and Blake, D.J. (2001) Dysbindin, a novel coiled-coil-containing protein that interacts with the dystrobrevins in muscle and brain. *J. Biol. Chem.*, **276**, 24232–24241.
18. Turner, K.M., Burgoyne, R.D. and Morgan, A. (1999) Protein phosphorylation and the regulation of synaptic membrane traffic. *Trends. Neurosci.*, **22**, 459–464.
19. Brunet, A., Datta, S.R. and Greenberg, M.E. (2001) Transcription-dependent and -independent control of neuronal survival by the PI3K-Akt signaling pathway. *Curr. Opin. Neurobiol.*, **11**, 297–305.
20. Numakawa, T., Nakayama, H., Suzuki, S., Kubo, T., Nara, F., Numakawa, Y., Yokomaku, D., Araki, T., Ishimoto, T., Ogura, A. *et al.* (2003) Nerve growth factor-induced glutamate release is via p75 receptor, ceramide, and Ca(2+) from ryanodine receptor in developing cerebellar neurons. *J. Biol. Chem.*, **278**, 41259–41269.
21. Williams, N.M., Preece, A., Morris, D.W., Spurlock, G., Bray, N.J., Stephens, M., Norton, N., Williams, H., Clement, M., Dwyer, S. *et al.* (2004) Identification in 2 independent samples of a novel schizophrenia risk haplotype of the dystrobrevin binding protein gene (*DTNBP1*). *Arch. Gen. Psychiatr.*, **61**, 336–344.
22. Tokuhiro, S., Yamada, R., Chang, X., Suzuki, A., Kochi, Y., Sawada, T., Suzuki, M., Nagasaki, M., Ohtsuki, M., Ono, M. *et al.* (2003) An intronic SNP in a RUNX1 binding site of SLC22A4, encoding an organic cation transporter, is associated with rheumatoid arthritis. *Nat. Genet.*, **35**, 341–348.
23. McClintock, W., Shannon Weickert, C., Halim, N.D., Lipska, B.K., Hyde, T.M., Herman, M.M., Weinberger, D.R., Kleinman, J.E. and Straub, R.E. (2003) Reduced expression of dysbindin protein in the dorsolateral prefrontal cortex of patients with schizophrenia. *Program No. 317.9. 2003 Abstract Viewer/Itinerary Planner.* Washington, DC, Society for Neuroscience (Online).
24. Talbot, K., Eidem, W.L., Tinsley, C.L., Benson, M.A., Thompson, E.W., Smith, R.J., Hahn, C.G., Siegel, S.J., Trojanowski, J.Q., Gur, R.E. *et al.* (2004) Dysbindin-1 is reduced in intrinsic, glutamatergic terminals of the hippocampal formation in schizophrenia. *J. Clin. Invest.*, **113**, 1353–1363.
25. Weickert, C.S., Straub, R.E., McClintock, B.W., Matsumoto, M., Hashimoto, R., Hyde, T.M., Herman, M.M., Weinberger, D.R. and Kleinman, J.E. (2004) Human dysbindin (*DTNBP1*) gene expression in normal brain and in schizophrenic prefrontal cortex and midbrain. *Arch. Gen. Psychiatr.*, **61**, 544–555.
26. Honer, W.G., Falkai, P., Bayer, T.A., Xie, J., Hu, L., Li, H.Y., Arango, V., Mann, J.J., Dwork, A.J. and Trimble, W.S. (2002) Abnormalities of SNARE mechanism proteins in anterior frontal cortex in severe mental illness. *Cereb. Cortex*, **12**, 349–356.
27. Vawter, M.P., Thatcher, L., Usen, N., Hyde, T.M., Kleinman, J.E. and Freed, W.J. (2002) Reduction of synapsin in the hippocampus of patients with bipolar disorder and schizophrenia. *Mol. Psychiatr.*, **7**, 571–578.
28. Emamian, E.S., Hall, D., Birnbaum, M.J., Karayiorgou, M. and Gogos, J.A. (2004) Convergent evidence for impaired AKT1-GSK3beta signaling in schizophrenia. *Nat. Genet.*, **36**, 131–137.
29. Li, W., Zhang, Q., Oiso, N., Novak, E.K., Gautam, R., O'Brien, E.P., Tinsley, C.L., Blake, D.J., Spritz, R.A., Copeland, N.G. *et al.* (2003) Hermansky–Pudlak syndrome type 7 (HPS-7) results from mutant dysbindin, a member of the biogenesis of lysosome-related organelles complex 1 (BLOC-1). *Nat. Genet.*, **35**, 84–89.
30. Hashimoto, R., Yoshida, M., Ozaki, N., Yamanouchi, Y., Iwata, N., Suzuki, T., Kitajima, T., Tatsumi, M., Kamijima, K. and Kunugi, H. (2004) Association analysis of the −308G>A promoter polymorphism of the tumor necrosis factor alpha (TNF-alpha) gene in Japanese patients with schizophrenia. *J. Neural Transm.*, **111**, 217–221.
31. Hashimoto, R., Straub, R.E., Weickert, C.S., Hyde, T.M., Kleinman, J.E. and Weinberger, D.R. (2004) Expression analysis of neuregulin-1 in the dorsolateral prefrontal cortex in schizophrenia. *Mol. Psychiatr.*, **9**, 299–307.
32. Numakawa, T., Matsumoto, T., Adachi, N., Yokomaku, D., Kojima, M., Takei, N. and Hatanaka, H. (2001) Brain-derived neurotrophic factor triggers a rapid glutamate release through increase of intracellular Ca(2+) and Na(+) in cultured cerebellar neurons. *J. Neurosci. Res.*, **66**, 96–108.
33. Numakawa, T., Yamagishi, S., Adachi, N., Matsumoto, T., Yokomaku, D., Yamada, M. and Hatanaka, H. (2002) Brain-derived neurotrophic factor-induced potentiation of Ca(2+) oscillations in developing cortical neurons. *J. Biol. Chem.*, **277**, 6520–6529.
34. Kawamura, M., Namba, H., Otsu, Y., Hayashi, Y., Takei, N. and Nawa, H. (2003) Characterization of novel bicistronic sindbis virus vectors, SinEGdsp and SinIRES-EG, in cultured neurons. *Recent Res. Dev. Neurochem.*, **6**, 105–120.
35. Numakawa, T., Yokomaku, D., Kiyosue, K., Adachi, N., Matsumoto, T., Numakawa, Y., Taguchi, T., Hatanaka, H. and Yamada, M. (2002) Basic fibroblast growth factor evokes a rapid glutamate release through activation of the MAPK pathway in cultured cortical neurons. *J. Biol. Chem.*, **277**, 28861–28869.
36. Hashimoto, R., Nakamura, Y., Komai, S., Kashiwagi, Y., Tamura, K., Goto, T., Aimoto, S., Kaibuchi, K., Shiosaka, S. and Takeda, M. (2000) Site-specific phosphorylation of neurofilament-L is mediated by calcium/calmodulin-dependent protein kinase II in the apical dendrites during long-term potentiation. *J. Neurochem.*, **75**, 373–382.
37. Good, P. (2000) *Permutation Tests. A Practical Guide to Resampling Methods for Testing Hypothesis.* 2nd edn. Springer-Verlag, New York.

Journal of Neurochemistry, 2004, **91**, 299–307 doi:10.1111/j.1471-4159.2004.02713.x

U-box protein carboxyl terminus of Hsc70-interacting protein (CHIP) mediates poly-ubiquitylation preferentially on four-repeat Tau and is involved in neurodegeneration of tauopathy

Shigetsugu Hatakeyama,*,‡ Masaki Matsumoto,*,‡ Takumi Kamura,*,‡ Miyuki Murayama,¶ Du-Hua Chui,¶ Emmanuel Planel,¶ Ryosuke Takahashi,§ Keiichi I. Nakayama*,†,‡ and Akihiko Takashima¶

**Department of Molecular and Cellular Biology and †Department of Molecular Genetics, Medical Institute of Bioregulation, Fukuoka, Japan*

‡CREST, Japan Science and Technology Corporation, Saitama, Japan

§Laboratory for Motor System Neurodegeneration and ¶Laboratory for Alzheimer's Disease, Brain Science Institute, RIKEN, Saitama, Japan

Abstract

Neurofibrillary tangles (NFTs), which are composed of hyperphosphorylated and ubiquitylated tau, are exhibited at regions where neuronal loss occurs in neurodegenerative diseases; however, the mechanisms of NFT formation remain unknown. Molecular studies of frontotemporal dementia with parkinsonism-17 demonstrated that increasing the ratio of tau with exon 10 insertion induced fibrillar tau accumulation. Here, we show that carboxyl terminus of Hsc70-interacting protein (CHIP), a U-box protein, recognizes the microtubule-binding repeat region of tau and preferentially ubiquitylates four-repeat tau compared with three-repeat tau. Overexpression of CHIP induced the prompt degradation of tau, reduced the formation of detergent-insoluble tau and inhibited proteasome inhibitor-induced cell death. NFT bearing neurons in progressive supranuclear palsy, in which four-repeat tau is a component, showed the accumulation of CHIP. Thus, CHIP is a ubiquitin ligase for four-repeat tau and maintains neuronal survival by regulating the quality control of tau in neurons.

Keywords: carboxyl terminus of Hsc70-interacting protein, neurodegeneration, neurofibrillary tangle, tau, ubiquitylation.

J. Neurochem. (2004) **91**, 299–307.

Protein aggregation causes the pathological lesions associated with neurodegenerative disorders (Kopito and Ron 2000). Neurofibrillary tangles (NFTs) emerge when pathological tau protein aggregates accumulate in neurons and form paired helical filament-tau proteins. These aggregates are composed of both ubiquitylated and highly phosphorylated tau and are characteristic of several neurodegenerative diseases, including Alzheimer's disease (Selkoe 2000; Lee *et al.* 2001; Hardy and Selkoe 2002). Of the several kinases that play a role in the hyperphosphorylation of paired helical filament-tau (Ishiguro *et al.* 1993; Morishima-Kawashima *et al.* 1995; Goedert *et al.* 1997), GSK-3β and JNK hyperphosphorylation leads to the formation of paired helical filament-like, detergent-insoluble tau (Sato *et al.* 2002). Tau gene mutations have recently been reported to cause frontotemporal dementia with parkinsonism-17, which has been characterized as exhibiting NFTs and neuron loss without β-amyloid peptide deposition in autopsied human brains, demonstrating that tau abnormalities alone can cause NFTs and neuronal death. While exonic mutations, such as P301L, affect the biochemical nature of tau and promote the self-assembly of mutant tau into filaments, intronic mutations within exon 10 or its 5′ splice regulatory region alter the ratio

Received January 19, 2004; revised manuscript received May 27, 2004; accepted June 11, 2004.

Address correspondence and reprint requests to Akihiko Takashima, Laboratory for Alzheimer's Disease, Brain Science Institute, RIKEN, Saitama 351-0198, Japan. E-mail: kenneth@brain.riken.jp

Abbreviations used: AD, Alzheimer's disease; CHIP, carboxyl terminus of Hsc70-interacting protein; EGFP, enhanced green fluorescent protein; GFP, green fluorescent protein; GST, glutathione S-transferase; HA, haemaglutinin; IB, immunoblot; IP, immunoprecipitate; NFT, neurofibrillary tangle; RNAi, RNA interference; SDS, sodium dodecyl sulfate; TPR, tetratricopeptide repeat; WCE, whole cell lysate.

of tau isoforms. In general, these mutations affect exon 10 splicing patterns thus altering the relative proportions of four- and three-repeat tau that are expressed. An increase in four-repeat tau induces the accumulation of four-repeat tau and NFT formation. We assumed that an impairment in a mechanism for four-repeat tau degradation would lead to four-repeat tau accumulation. As tau in NFTs is ubiquitylated, the ubiquitin proteasome may be the mechanism responsible for tau degradation in neurodegeneration (Mori *et al.* 1987) and the deterioration of this system might contribute to NFT formation. However, the mechanism by which the ubiquitylation of tau occurs is still unknown.

Protein ubiquitylation is mediated by a multienzyme cascade involving at least three distinct types of enzymes, a ubiquitin-activating enzyme (E1), a ubiquitin-conjugating enzyme (E2) and a ubiquitin-protein ligase (E3) (Hershko 1983). E3 enzymes catalyse the final step for substrate recognition in the ubiquitylation pathway. Currently there are two known E3 ligases, the HECT family E3s and adaptor E3s containing a RING finger or a U-box (Weissman 2001; Hatakeyama and Nakayama 2003). The carboxyl terminus of Hsc70-interacting protein (CHIP) has a U-box domain and was originally identified as a tetratricopeptide repeat (TPR)-containing protein that interacts with mammalian heat shock protein Hsc/Hsp70 (Ballinger *et al.* 1999). CHIP binds directly to the molecular chaperones Hsp90 or Hsc70 via TPR domains; therefore, when unfolded or misfolded proteins accumulate, CHIP may contribute to the cellular response. The combination of CHIP and Hsp90 mediates the ubiquitylation of the glucocorticoid receptor and CHIP with Hsc70 targets the immature cystic fibrosis transmembrane conductance regulator for proteasomal degradation (Connell *et al.* 2001; Meacham *et al.* 2001). We recently showed that the level of Hsp90 is reduced in tau-accumulated neurons of Tg mice expressing frontotemporal dementia with parkinsonism-17 tau mutations (Tanemura *et al.* 2001, 2002; Tatebayashi *et al.* 2002; Dou *et al.* 2003). This prompted us to investigate the possible involvement of CHIP in the poly-ubiquitylation of tau.

Materials and methods

Cell culture

HEK293T, COS7 or Neuro2A cells were cultured under an atmosphere of 5% CO_2 at 37°C in Dulbecco's modified Eagle's medium (Invitrogen; Carlsbad, CA, USA) supplemented with 10% fetal bovine serum (Invitrogen).

Cloning cDNAs and plasmid construction

The expression plasmids containing FLAG- or Myc-tagged mouse CHIP, mutants of these cDNAs [UFD2a, UFD2b, PRP19, IκBα, IKK2, haemaglutinin (HA)-tagged ubiquitin and wild type (four- and three-repeat)] and tau mutants were generated as previously described (Hatakeyama *et al.* 2001). To generate the mutant (P301L) of tau or Hsc70, we performed site-directed mutagenesis with a Quick Change kit (Stratagene, La Jolla, CA, USA) and with mutated oligonucleotide primers corresponding to each site.

Production of recombinant proteins in bacteria

Glutathione S-transferase (GST) fusion proteins were expressed in *Escherichia coli* strain DH5α cultured in the presence of 0.1 mM isopropyl-β-D-thiogalactopyranoside. Bacterial cells were resuspended in phosphate-buffered saline and lysed by sonication; cellular debris was removed by centrifugation for 20 min at 13 000 *g*. Glutathione-Sepharose 4B beads (Amersham Biosciences, Piscataway, NJ, USA) were added to the resulting supernatant fluid and the mixture was rotated at 4°C overnight. The beads were washed in phosphate-buffered saline and GST fusion proteins were eluted with 50 mM Tris-HCl (pH 8.0) containing 10 mM reduced glutathione.

Transfection, immunoprecipitation and immunoblot analysis

Cells were transfected using the calcium phosphate method and lysed in a lysis buffer containing 50 mM Tris-HCl (pH 7.4), 150 mM NaCl, 1% nonidet P-40, leupeptin (10 μg/mL), 1 mM phenylmethylsulfonyl fluoride, 400 μM Na_3VO_4, 400 μM EDTA, 1 mM EGTA, 10 mM NaF and 10 mM sodium pyrophosphate. The lysate was centrifuged at 16 000 *g* for 10 min at 4°C and the resulting supernatant fluid was incubated with antibodies for 2 h at 4°C. Protein G-Sepharose equilibrated in the same buffer was added to the mixture, which was then rotated for 1 h at 4°C. The resin was separated by centrifugation, washed four times with lysis buffer and then boiled in sodium dodecyl sulfate (SDS) sample buffer. Immunoblot analysis was performed with the following primary antibodies: anti-Myc (1 μg/mL; 9E10, Covance Inc., Princeton, NJ, USA), anti-FLAG (1 μg/mL; M5, Sigma-Aldrich, St. Louis, MO, USA), anti-HA (1 μg/mL; HA.11/16B12, Babco, Berkeley, CA, USA), anti-Hsp90 (1 μg/mL; 68, Transduction Laboratories, San Jose, CA, USA), anti-Hsp70 (1 μg/mL; 7, Transduction Laboratories), anti-CHIP (1 μg/mL, Hatakeyama and Nakayama 2003), $p27^{Kip1}$ (1 μg/mL; 57, Transduction Laboratories) and anti-ubiquitin (1 μg/mL; 1B3, MBL International, Woburn, MA, USA). Immune complexes were detected with horseradish peroxidase-conjugated antibodies to mouse or rabbit immunoglobulin G (1 : 10 000 dilution; Promega Corporation, Madison, WI, USA) and an enhanced chemiluminescence system (ECL; Amersham Biosciences).

Isolation of insoluble tau from cell lines

Cells were lysed with ristocetin-induced platelet agglutination buffer containing 1% SDS. Cell lysate (2 mg) was centrifuged for 20 min at 100 000 *g* at 4°C. The resulting pellet was washed four times with 300 μL of ristocetin-induced platelet agglutination buffer using a sonic homogenizer. The insoluble pellet was solubilized in 70% formic acid for use in the immunoblot analysis or resuspended in 100 mM Tris-HCl (pH 8.3) for examination using electron microscopy. Following centrifugation for 20 min at 100 000 *g* at 4°C, the formic acid fraction was collected, air-dried and subjected to immunoblot analysis after suspension in SDS gel loading buffer. The samples were resolved on SDS–polyacrylamide gel electrophoresis and immunoblot analysis was performed.

In vitro ubiquitylation assay

The *in vitro* ubiquitylation assay was performed as described previously (Hatakeyama *et al.* 2001). In brief, reaction mixtures (20 μL) containing 1 μg of recombinant GST-CHIP, 0.1 μg of recombinant rabbit E1 (Boston Biomedica, Boston, MA, USA), 1 μL of recombinant human Ubc4, 0.5 U of phosphocreatine kinase, 1 μg of GST-Ub (MBL), 25 mM Tris-HCl (pH 7.5), 120 mM NaCl, 2 mM ATP, 1 mM $MgCl_2$, 0.3 mM dithiothreitol and 1 mM creatine phosphate were incubated for 2 h at 30°C. The reaction was terminated by the addition of SDS sample buffer containing 4% 2ME and heating at 95°C for 5 min. Samples were resolved by SDS–polyacrylamide gel electrophoresis on a 6% gel and then subjected to immunoblot analysis with a mouse monoclonal antibody to tau (clone 15; Transduction Laboratories) and horseradish peroxidase-conjugated rabbit polyclonal antibody to mouse Ig (Promega). Signals were detected with ECL (Amersham Pharmacia).

Pulse-chase analysis with cycloheximide

Cells were cultured with cycloheximide at a concentration of 50 μg/mL and then incubated for various times. Cell lysates were then subjected to SDS–polyacrylamide gel electrophoresis and immunoblot analysis with antibody to Myc, Hsp90, FLAG and $p27^{Kip1}$.

RNA interference and retroviral infection

The retroviral expression vector, which encodes the double-stranded RNA corresponding to nucleotides 864–883 of the mouse CHIP coding region or to enhanced green fluorescent protein (EGFP), was constructed using pMX-puro, kindly provided by Dr Kitamura (Osaka University, Graduate School of Medicine, Osaka, Japan). For retrovirus-mediated gene expression, Neuro2A cells were infected with retroviruses produced by Plat-E packaging cells and then cultured in the presence of 0.2 μg/mL puromycin (Sigma). pMX-neo vector was used for Myc-tau (P301L).

Induction and detection of cell death

Stable Neuro2A cell lines were cultured with 20 μM MG132 (Peptide Institute, Osaka, Japan) and incubated for 24 h; the cell number was counted after trypan blue staining.

Immunohistotochemical staining

Brains were immersion fixed with 10% buffered formalin and paraffin-embedded sections (2–10 μm) were prepared for confocal microscopic analyses. Deparaffinized sections were treated in either 0.1% Triton X-100 in phosphate-buffered saline for 20 min or Target Retrieval Solution (Dako Cytomation Denmark A/S, Glostrop, Denmark). AT8 and anti-CHIP were used as primary antibodies and then incubated with either Alexa488/568-conjugated anti-mouse IgG or Alexa488/568-conjugated anti-rabbit IgG. Sections were then examined with a Radiance 2000 KR3 confocal microscope (Bio-Rad Laboratories, Hercules, CA, USA).

Results

We first examined the involvement of U-box proteins in tau ubiquitylation. The overexpression of UFD2a, UFD2b or PRP19 U-box proteins had no effect on tau ubiquitylation compared with control, which showed only minimal tau ubiquitylation with endogenous E3 ligases (Fig. 1a). Only CHIP overexpression exhibited poly-ubiquitylated tau (Fig. 1a), suggesting that CHIP participates in this ubiquitylation process. To confirm this result, various combinations of tau, Myc-CHIP and HA-tagged ubiquitin were expressed in COS7 cells and tau was purified from the heat-stable materials of each cell lysate by immunoprecipitation using an anti-tau antibody. Tau from Myc-CHIP- and HA-tagged ubiquitin-coexpressing cells revealed anti-HA immunoreactivity, suggesting that tau protein is covalently modified by ubiquitin under the expression of CHIP (Fig. 1b). This result was verified by purifying ubiquitylated protein from CHIP- and tau-expressing cells. Using an Ni column, ubiquitylated proteins were purified from cells expressing tau, histidine-tagged Ub with or without CHIP. CHIP expression greatly enhanced the recovery of ubiquitylated tau in elution fractions 1 and 2 (Fig. 1c) and the ubiquitylated tau by CHIP was about 3.4% of total tau. Thus, CHIP is an E3-ubiquitin ligase for tau and the overexpression of CHIP increases tau ubiquitylation in an *in vivo* system. To further confirm the ubiquitylation of tau by CHIP, we reconstituted ubiquitylated tau in an *in vitro* ubiquitylation assay with these recombinants; E1, E2 (UbcH5C), GST-ubiquitin (GST-Ub), GST-CHIP and His-tau were required for tau ubiquitylation (Fig. 1d). Unexpectedly, chaperone proteins, phosphorylated tau or other such factors were not required for tau ubiquitylation by CHIP. Thus, these results indicated that CHIP alone can ubiquitylate even non-phosphorylated tau *in vitro*.

To test the interaction between tau and CHIP *in vivo*, mutants with CHIP and tau deletions (Fig. 2) were prepared and expressed in HEK293 or COS7 cells. Full-length tau could bind to full-length CHIP but not to CHIP (ΔU) lacking a U-box domain, CHIP (ΔTPR) lacking a TPR or CHIP (ΔCU) lacking both the charged region and U-box (Fig. 2a). Conversely, full-length CHIP could associate with full-length tau (four-repeat) and with the region lacking the N-terminus of tau (R-C) but not with the region lacking the repeat regions (ΔR) (Fig. 2b). These findings suggest that CHIP associates with the microtubule-binding repeat regions of tau. We further investigated the interaction and ubiquitylation of CHIP on four- and three-repeat tau (Fig. 2c). Three-repeat tau was less efficiently ubiquitylated by CHIP (Fig. 2d) and the association of three-repeat tau and CHIP was much less than for four-repeat tau (Fig. 2c). Thus, CHIP might recognize around the second repeat region of tau, which corresponds to exon 10 and preferentially ubiquitylates four-repeat tau.

We next investigated the effects of CHIP on the stability of tau in Neuro2A cells stably expressing Myc-tau (P301L) and FLAG-CHIP (Fig. 3a). The stability of tau (P301L) was examined by cyclohexamide-chase analysis. After cycloheximide treatment, endogenous $p27^{Kip1}$ protein rapidly degraded (Fig. 3a, two blots from bottom) and endogenous HSP90 protein remained stable for over 30 h (Fig. 3a, third and

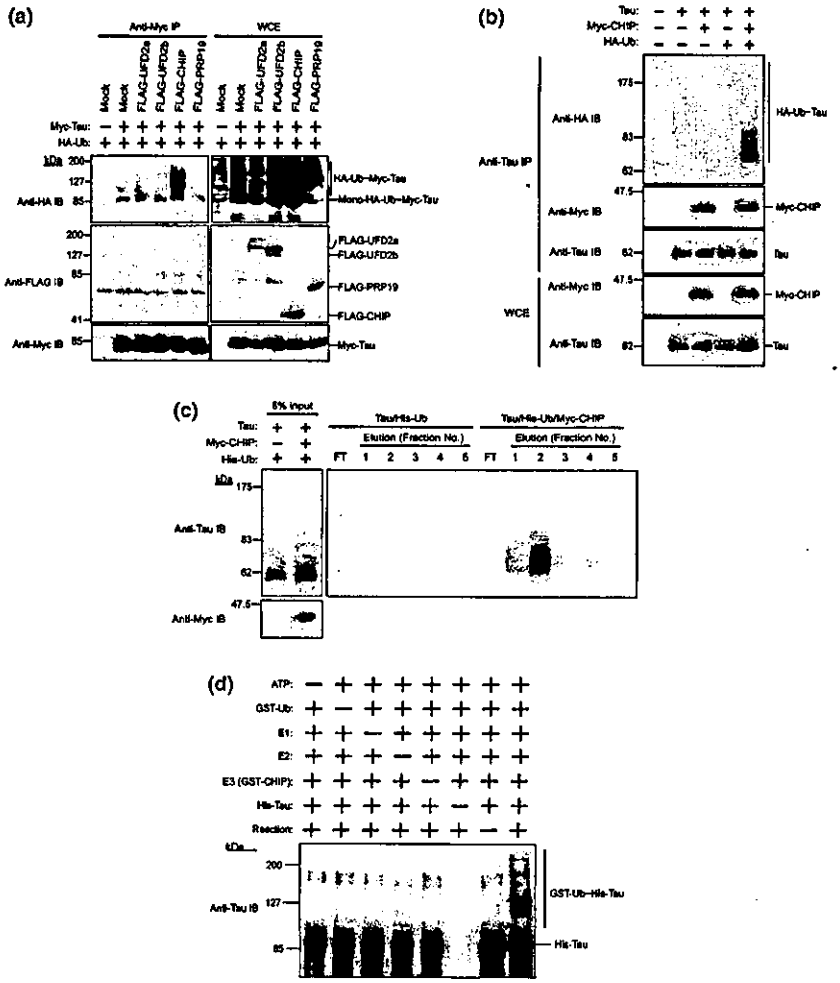

Fig. 1 Carboxyl terminus of Hsc70-interacting protein (CHIP) expression enhances the ubiquitylation on tau *in vivo*. (a) Specific ubiquitin ligase activity of CHIP for tau. The expression vectors for FLAG-UFD2a, -UFD2b, -CHIP, -PRP19, Myc-tagged human four-repeat tau and HA-tagged ubiquitin (HA-Ub) were transfected into HEK293T cells, the cell lysates were immunoprecipitated with anti-Myc monoclonal antibody and an anti-HA immunoblot was performed to detect the ubiquitylation on tau. Ten percent of cell lysates were used as WCE to detect the expression of each protein. (b) *In vivo* ubiquitylation assay for tau with CHIP. The expression vectors for Myc-CHIP, tau and HA-Ub were transfected into COS7 cells, the cell lysates were then immunoprecipitated with anti-tau monoclonal antibody and an anti-HA immunoblot was performed to detect the ubiquitylation on tau. Ten percent of cell lysates were used as WCE to detect the expression of each protein. (c) Fractionation of ubiquitylated tau from a cell expressing CHIP. The expression vectors for Myc-CHIP, tau and HA-Ub were transfected into COS7 cells, the cell lysates were then fractionated using an NI column and an anti-tau immunoblot was performed to detect the ubiquitylation on tau. Five percent of cell lysates were used as WCE to detect the expression of each protein. (d) *In vitro* ubiquitylation assay for tau with CHIP. Each component [ATP, glutathione S-transferase (GST)-Ub, E1, Ubc4, GST-CHIP and His-tau] was mixed, incubated at 30°C for 2 h, subjected to sodium dodecyl sulfate–polyacrylamide gel electrophoresis and then immunoblotted with anti-tau monoclonal antibody. IB, immunoblot; IP, immunoprecipitate; WCE, whole cell lysate.

fourth blots from top) when CHIP and tau were overexpressed together (Fig. 3a, third and seventh blots) and when tau alone was overexpressed (Fig. 3a, fourth and eighth blots from the top). Tau remained stable for over 30 h only in cells overexpressing tau (Fig. 3a, first blot), whereas the overexpression of CHIP enhanced tau degradation (Fig. 3a, second blot) without changing the exogenous expression level of CHIP (Fig. 3a, sixth blot from top). Moreover, tau ubiquitylated by CHIP accumulated when treated with the proteasome inhibitor lactacystin (Fig. 3b) These results suggest that CHIP induces the ubiquitylation of tau which is followed by degradation via proteasome. The effects of CHIP on the stability and ubiquitination of tau were not different between the P301L mutant and wild tau.

Knowing that CHIP recognizes and ubiquitylates tau and that this is followed by proteasome degradation, we investigated the role of CHIP in SDS-insoluble tau formation, one of the biochemical features of paired

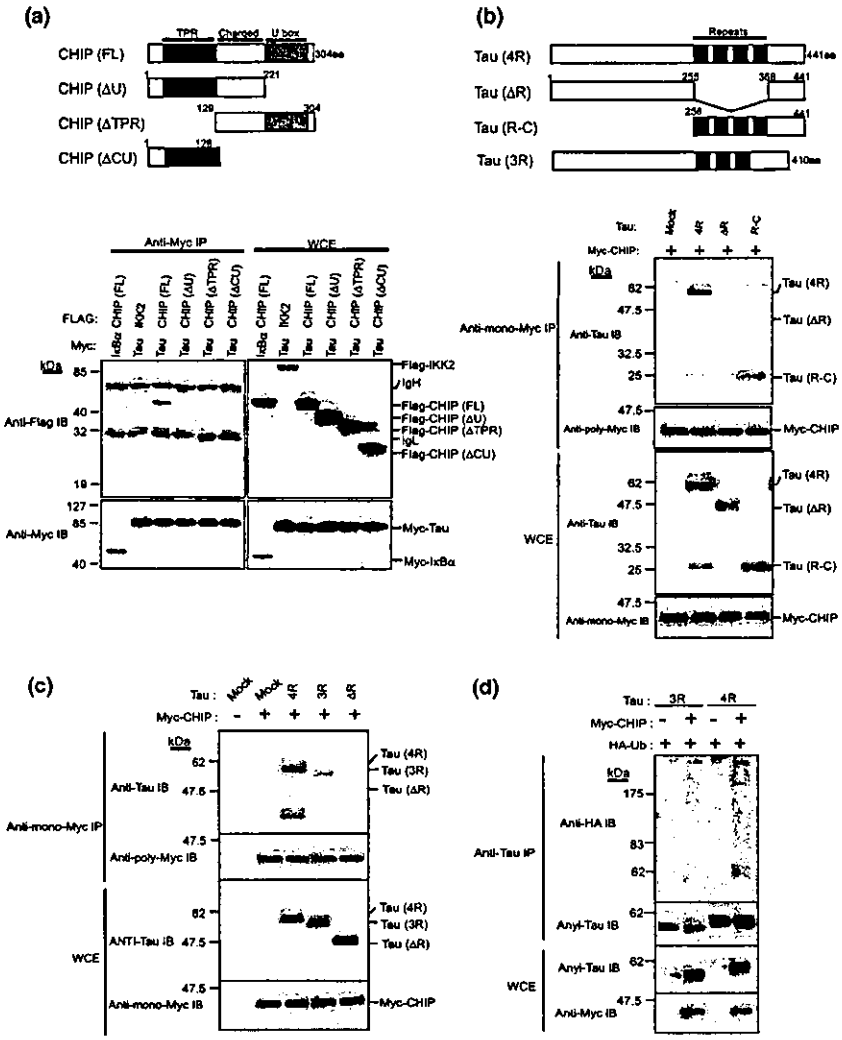

Fig. 2 Interaction between carboxyl terminus of Hsc70-interacting protein (CHIP) and four-repeat (4R) tau. (a) *In vivo* interaction between CHIP and tau. CHIP (FL) has the full-length (1–304) of CHIP. CHIP (ΔU), CHIP (ΔTPR) and CHIP (ΔCU) contain deletions of the U-box domain (222–304), tetratricopeptide repeat (TPR) domain (1–128) and charged region plus U-box domain (129–304), respectively. Black and gray boxes show the TPR and U-box domains, respectively. The expression vectors for full-length and mutants of FLAG-CHIP and Myc-tau (4R) were transfected into HEK293T cells, the cell lysates were immunoprecipitated with anti-Myc monoclonal antibody and anti-FLAG immunoblot was performed to detect the association with FLAG-CHIP or its mutants. Ten percent of cell lysates were used as WCE to detect the expression of each protein. Myc-IκBα and FLAG-IKK were used for negative controls. (b) Repeat domain of 4R tau interacts with CHIP. Tau (4R) is the longest form of 4R tau. Tau (ΔR) and tau (R-C) are the deletion of the 4R domain (256–441) and the N-terminal half (1–255), respectively. Black box shows repeat domain. The expression vectors for Myc-CHIP and truncated tau (4R) were transfected into COS7 cells, the cell lysates were immunoprecipitated with anti-Myc monoclonal antibody and anti-tau immunoblot was performed to detect the association with Myc-CHIP. The amount of immunoprecipitated CHIP was the same in all cell lysates (bottom panel). Ten percent of cell lysates were used as WCE to detect the expression of each protein. (c) Association of CHIP with 4R and three-repeat tau (3R). cDNAs described on the top of the blots were transfected into COS7 cells and cell lysates were immunoprecipitated using anti-myc antibody. Immunoprecipitants were probed by the anti-tau antibody TauC or anti-polyclonal antibody Myc. The amount of immunoprecipitated CHIP was the same in all cell lysates (bottom panel). (d) Ubiquitylation of 4R and 3R tau by CHIP. Each combination of cDNAs was transfected into COS7 cells. After immunoprecipitation of heat-stable materials using anti-tau antibody (HT7), immunoprecipitants were probed by anti-HA or tau C. The amount of immunoprecipitated tau was the same in all cell lysates (anti-tau IB panel in anti-tau IP panels) while the tau expression level was different.

helical filament-tau, using Neuro2A coexpressing frontotemporal dementia with parkinsonism-17 mutant tau (P301L) with or without FLAG-CHIP. The expression of P301L mutant tau induced the formation of SDS-insoluble tau and enhanced the recovery of tau in the SDS-insoluble fraction (formic acid-soluble fraction) by treatment with

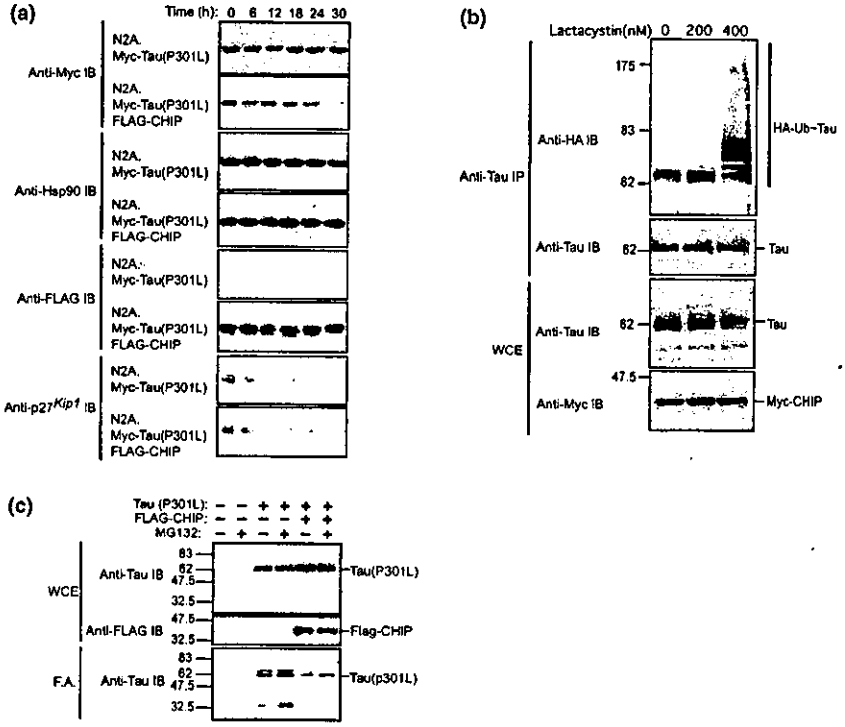

Fig. 3 Carboxyl terminus of Hsc70-interacting protein (CHIP) implicated in the regulation of neuronal cell death. (a) Cycloheximide-chase analysis of tau (P301L) with CHIP. The stably expressed Neuro2A cell lines with Myc-tau (P301L) and FLAG-CHIP were established by infection of retrovirus with cDNA encoding Myc-tau (P301L) and FLAG-CHIP and by puromycin selection. Cells were cultured with cycloheximide at a concentration of 50 μg/mL and then incubated for various times (0, 6, 12, 18, 24 and 30 h). Cell lysates were then subjected to sodium dodecyl sulfate–polyacrylamide gel electrophoresis (SDS–PAGE) and immunoblot analysis was performed with antibody to Myc, Hsp90, FLAG and $p27^{Kip1}$. The anti-$p27^{Kip1}$ immunoblot shows that cycloheximide is active. (b) Effects of treatment with the proteasome inhibitor lactacystin. HEK293 cells expressing tau, CHIP and HA-tagged ubiquitin (HA-Ub) were treated with various concentrations of lactacystin for 14 h, the cell lysates were immunoprecipitated with anti-tau monoclonal antibody and an anti-HA immunoblot was performed to detect the ubiquitylation on tau. (c) Soluble or insoluble fraction of Tau (P301L). The soluble (WCE) or insoluble [formic acid (FA)] fraction from cells expressing Tau (P301L) with or without FLAG-CHIP was separated with or without treatment with MG135. The fractions were subjected to SDS–PAGE and immunoblot analysis was performed with antibody to tau and FLAG. Hsp90 as internal control.

MG132, a potent inhibitor of proteasome (Fig. 3c, lanes 3 and 4). Coexpression with CHIP sustained the amount of the SDS-soluble tau fraction and significantly inhibited the formation of SDS-insoluble tau. MG132 treatment enhanced the formation of SDS-insoluble tau but the amount recovered was still much lower than that from cells where CHIP was not coexpressed (Fig. 3c, lanes 5 and 6). These results indicate that the inhibition of SDS-insoluble tau formation stems from the role of CHIP in the degradation of tau. Thus, CHIP may be involved in NFT formation.

Many suspect a possible connection between NFT formation and neuronal death in neurodegenerative diseases because neuronal loss is also common in areas where NFTs are observed. Therefore, we investigated the possible role of CHIP in connecting NFT formation and cell death. We first established cell lines that knocked down endogenous CHIP using a vector-based RNA interference (RNAi) technique (Fig. 4a). CHIP RNAi expression blocked the expression of endogenous CHIP but did not affect the expression of Hsp90. Green fluorescent protein (GFP) RNAi also did not affect CHIP expression. Tau (P301) over-expression had no affect on the cell viability of Neuro2A, even though SDS-insoluble tau was formed. Stable cell lines were incubated with the proteasome inhibitor MG132 (20 μM) for 24 h and then alive or dead cells were determined by trypan blue exclusion (Fig. 4b). This treatment induced cell death in 50% of the non-treated cells in GFP RNAi-expressing cells, CHIP-overexpressing cells and mock cells. The RNAi inhibition of CHIP and the expression of tau (P301L) facilitated an MG132-induced cell death of 70% of untreated cells and CHIP overexpression restored the cell death level to that of cells with no tau expression (Fig. 4b). Therefore, CHIP is involved in tau (P301L)-mediated, MG132-induced cell death. It should be noted that, although CHIP expression prevented neurons from undergoing proteasome inhibition-induced neuronal death, surviving neurons still showed SDS-insoluble tau (Fig. 3c) which suggests the development of

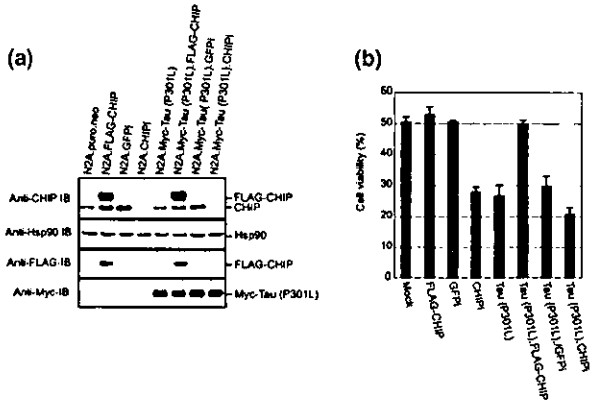

Fig. 4 Carboxyl terminus of Hsc70-interacting protein (CHIP) as a critical factor to protect from stress by proteasome inhibitor. (a) Reduced amounts of CHIP in cells with CHIP RNA interference (RNAi) but not EGFP RNAi. Neuro2A cells were treated with retrovirus vector-based RNAi for CHIP or EGFP and then selected with puromycin. These cell lines were further infected by retrovirus with Myc-tau (P031L) and neo^R and then selected with puromycin and G418. Double-infected cell lines were used for immunoblot with antibodies to CHIP, FLAG, Myc and Hsp90 as internal control. (b) Stable Neuro2A cell lines were cultured with 20 μM MG132, incubated for 24 h and the cell number was counted after trypan blue staining. The amounts of CHIP in cells with CHIP but not EGFP RNAi were reduced. Neuro2A cells were treated with retrovirus vector-based RNAi for CHIP or EGFP and then selected with puromycin.

NFT formation. This was verified by neuropathological staining in which CHIP colocalized in NFTs of progressive supranuclear palsy brain (Fig. 5), mostly containing four-repeat tau, and also reacted to anti-ubiquitin antibody. The most NFT-bearing cells were stained by the anti-CHIP antibody in progressive supranuclear palsy brain but very faintly stained in Alzheimer's disease (AD) brain (data not shown).

Discussion

In this study, we have shown that the U-box protein CHIP is a tau-interacting protein *in vivo* and that CHIP mediates poly-ubiquitylation preferentially on four-repeat tau as a ubiquitin ligase followed by degradation by proteasome. In the *in vitro* ubiquitination assay, molecular chaperones such as Hsp90 or Hsc70 or hyperphosphorylation of tau are not required for CHIP-mediated tau ubiquitylation (Fig. 1d). To date, CHIP has been shown to bind to a subset of chaperone substrates, including glucocorticoid receptor, cystic fibrosis transmembrane conductance regulator and ErbB2, suggesting that CHIP has sensor functions that recognize different kinds of misfolded proteins (Connell *et al.* 2001; Meacham *et al.* 2001; Imai *et al.* 2002; Xu *et al.* 2002). In *in vivo* conditions, Hsp might support the CHIP-mediated tau ubiquitylation and degradation because tau was not accumulated in neurons exhibiting an increased level of Hsp90 (Dou *et al.* 2003). To

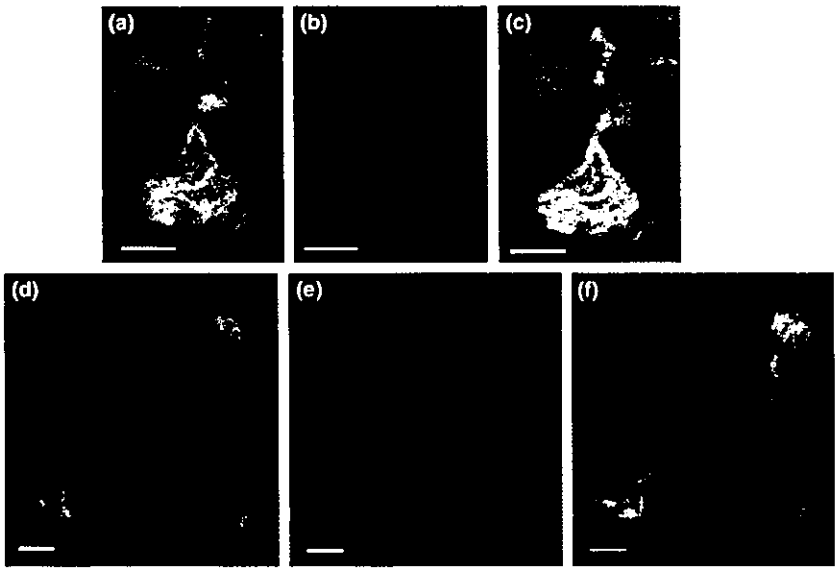

Fig. 5 Neuropathological analysis in progressive supranuclear palsy (PSP). Neurons in PSP brain were stained with anti-carboxyl terminus of Hsc70-interacting protein (CHIP; green; a and d) and anti-phosphorylated tau (AT8; orange; b and e). (c and f) Merged image of both anti-CHIP and AT8 immunoreactivities. Brains were immersion fixed with 10% buffered formalin and paraffin-embedded sections (2–10 μm) were prepared for confocal microscopic analyses. Deparaffinized sections were treated in either 0.1% Triton X-100 in phosphate-buffered saline for 20 min or Target Retrieval Solution (Dako). AT8 and anti-CHIP were used as primary antibodies and then incubated with either Alexa488/568-conjugated anti-mouse IgG or Alexa488/568-conjugated anti-rabbit IgG. Sections were then examined with a Radiance 2000 KR3 confocal microscope (Bio-Rad). Scale bars, 10 μm.

uncover how CHIP recognizes and ubiquitylates tau without molecular chaperones, it is first necessary to understand the structural basis for this significant function.

Phosphorylated tau was reported to preferentially ubiquitylate in COS cells (Shimura *et al.* 2003). In our experiments, four-repeat tau was ubiquitylated by CHIP without phosphorylation. This discrepancy might be due to the different purification procedures for ubiquitylated tau and/or the different tau cDNA used. Shimura *et al.* (2003) used EGFP-tagged tau. As recombinant tau, which was not phosphorylated, could be ubiquitylated in an *in vitro* reconstitution system, CHIP must recognize and ubiquitylate both non-phospho and phospho tau.

The ubiquitinated tau found in AD brains was recovered in the SDS-insoluble fraction, suggesting that its ubiquitylation may precede fibril formation. A large amount of SDS-insoluble tau was recovered in P301L mutant tau-expressing cells in the present study and MG132 treatment enhanced the accumulation of tau in the SDS-insoluble fraction, suggesting that tau (P301L) is degraded by the ubiquitin–proteasome system. CHIP overexpression reduced the recovery of tau in the SDS-insoluble fraction and MG132 treatment showed only a small increase of SDS-insoluble tau, suggesting that the ubiquitylation of tau occurs before tau acquires insolubility against SDS. An inhibition of proteasome activity in the AD brain has been reported previously (Goldbaum *et al.* 2003; Keck *et al.* 2003). Taken together with the MG132-induced cytotoxicity of P301L tau overexpression, these results suggest that tau accumulation in the SDS-insoluble fraction itself was not toxic but rather that the neurons exhibited vulnerability against the stress of protein accumulation by inhibition of proteasome. CHIP expression reduces the stress induced by this cytotoxicity by reducing the amount of SDS-insoluble tau. Therefore, although CHIP-expressing neurons survive, ubiquitynated tau might remain in some neurons and develop into NFTs.

Acknowledgements

We thank S. Matsushita, K. Shinohara, N. Nishimura, R. Yasukouchi and other laboratory members for technical assistance and C. Sugita and M. Kimura for help in preparing the manuscript. This work was supported in part by a grant from the Ministry of Education, Science, Sports and Culture of Japan and by YASUDA Medical Research Foundation (SH).

References

Ballinger C. A., Connell P., Wu Y., Hu Z., Thompson L. J., Yin L. Y. and Patterson C. (1999) Identification of CHIP, a novel tetratricopeptide repeat-containing protein that interacts with heat shock proteins and negatively regulates chaperone functions. *Mol. Cell. Biol.* **19**, 4535–4545.

Connell P., Ballinger C. A., Jiang J., Wu Y., Thompson L. J., Hohfeld J. and Patterson C. (2001) The co-chaperone CHIP regulates protein triage decisions mediated by heat-shock proteins. *Nat. Cell Biol.* **3**, 93–96.

Dou F., Netzer W. J., Tanemura K., Li F., Hartl F. U., Takashima A., Gouras G. K., Greengard P. and Xu H. (2003) Chaperones increase association of tau protein with microtubules. *Proc. Natl Acad. Sci. USA* **100**, 721–726.

Goedert M., Hasegawa M., Jakes R., Lawler S., Cuenda A. and Cohen P. (1997) Phosphorylation of microtubule-associated protein tau by stress-activated protein kinases. *FEBS Lett.* **409**, 57–62.

Goldbaum O., Oppermann M., Handschuh M., Dabir D., Zhang B., Forman M. S., Trojanowski J. Q., Lee V. M. and Richter-Landsberg C. (2003) Proteasome inhibition stabilizes tau inclusions in oligodendroglial cells that occur after treatment with okadaic acid. *J. Neurosci.* **23**, 8872–8880.

Hardy J. and Selkoe D. J. (2002) The amyloid hypothesis of Alzheimer's disease: progress and problems on the road to therapeutics. *Science* **297**, 353–356.

Hatakeyama S. and Nakayama K. I. (2003) U-box proteins as a new family of ubiquitin ligases. *Biochem. Biophys. Res. Commun.* **302**, 635–645.

Hatakeyama S., Yada M., Matsumoto M., Ishida N. and Nakayama K. I. (2001) U box proteins as a new family of ubiquitin-protein ligases. *J. Biol. Chem.* **276**, 33 111–33 120.

Hershko A. (1983) Ubiquitin: roles in protein modification and breakdown. *Cell* **34**, 11–12.

Imai Y., Soda M., Hatakeyama S., Akagi T., Hashikawa T., Nakayama K. and Takahashi R. (2002) CHIP is associated with Parkin, a gene responsible for familial Parkinson's disease, and enhances its ubiquitin ligase activity. *Mol. Cell* **10**, 55–67.

Ishiguro K., Shiratsuchi A., Sato S., Omori A., Arioka M., Kobayashi S., Uchida T. and Imahori K. (1993) Glycogen synthase kinase 3 beta is identical to tau protein kinase I generating several epitopes of paired helical filaments. *FEBS Lett.* **325**, 167–172.

Keck S., Nitsch R., Grune T. and Ullrich O. (2003) Proteasome inhibition by paired helical filament-tau in brains of patients with Alzheimer's disease. *J. Neurochem.* **85**, 115–122.

Kopito R. R. and Ron D. (2000) Conformational disease. *Nat. Cell Biol.* **2**, E207–E209.

Lee V. M., Goedert M. and Trojanowski J. Q. (2001) Neurodegenerative tauopathies. *Annu. Rev. Neurosci.* **24**, 1121–1159.

Meacham G. C., Patterson C., Zhang W., Younger J. M. and Cyr D. M. (2001) The Hsc70 co-chaperone CHIP targets immature CFTR for proteasomal degradation. *Nat. Cell Biol.* **3**, 100–105.

Mori H., Kondo J. and Ihara Y. (1987) Ubiquitin is a component of paired helical filaments in Alzheimer's disease. *Science* **235**, 1641–1644.

Morishima-Kawashima M., Hasegawa M., Takio K., Suzuki M., Yoshida H., Titani K. and Ihara Y. (1995) Proline-directed and non-proline-directed phosphorylation of PHF-tau. *J. Biol. Chem.* **270**, 823–829.

Sato S., Tatebayashi Y., Akagi T. *et al.* (2002) Aberrant tau phosphorylation by glycogen synthase kinase-3beta and JNK3 induces oligomeric tau fibrils in COS-7 cells. *J. Biol. Chem.* **277**, 42 060–42 065.

Selkoe D. J. (2000) Toward a comprehensive theory for Alzheimer's disease. Hypothesis: Alzheimer's disease is caused by the cerebral accumulation and cytotoxicity of amyloid beta-protein. *Ann. NY Acad. Sci.* **924**, 17–25.

Shimura H., Schwartz D., Gygi S. P. and Kosik K. S. (2004) CHIP-Hsc70 complex ubiquitinates phosphorylated Tau and enhances cell survival. *J. Biol. Chem.* **279**, 4869–4876.

Tanemura K., Akagi T., Murayama M. *et al.* (2001) Formation of filamentous tau aggregations in transgenic mice expressing V337M human tau. *Neurobiol. Dis.* **8**, 1036–1045.

Tanemura K., Murayama M., Akagi T., Hashikawa T., Tominaga T., Ichikawa M., Yamaguchi H. and Takashima A. (2002) Neurode-

generation with tau accumulation in a transgenic mouse expressing V337M human tau. *J. Neurosci.* **22**, 133–141.

Tatebayashi Y., Miyasaka T., Chui D. H. *et al.* (2002) Tau filament formation and associative memory deficit in aged mice expressing mutant (R406W) human tau. *Proc. Natl Acad. Sci. USA* **99**, 13 896–13 901.

Weissman A. M. (2001) Themes and variations on ubiquitylation. *Nat. Rev. Mol. Cell Biol.* **2**, 169–178.

Xu W., Marcu M., Yuan X., Mimnaugh E., Patterson C. and Neckers L. (2002) Chaperone-dependent E3 ubiquitin ligase CHIP mediates a degradative pathway for c-ErbB2/Neu. *Proc. Natl Acad. Sci. USA* **99**, 12 847–12 852.

Journal of Neuroscience Research 75:417–428 (2004)

Amino- and Carboxyl-Terminal Mutants of Presenilin 1 Cause Neuronal Cell Death Through Distinct Toxic Mechanisms: Study of 27 Different Presenilin 1 Mutants

Yuichi Hashimoto,[1] Emi Tsukamoto,[1] Takako Niikura,[1] Yohichi Yamagishi,[1] Miho Ishizaka,[1] Sadakazu Aiso,[2] Akihiko Takashima,[3] and Ikuo Nishimoto[1]*

[1]Department of Pharmacology, KEIO University School of Medicine, Tokyo, Japan
[2]Department of Anatomy, KEIO University School of Medicine, Tokyo, Japan
[3]Laboratory for Alzheimer's Disease, Brain Science Institute, RIKEN, Saitama, Japan

Presenilin (PS)1 and its mutants, which consist of the N-terminal and C-terminal fragments, cause certain familial forms of Alzheimer's disease (FAD). Our earlier studies found that FAD-linked M146L-PS1 causes neuronal cell death through nitrogen oxide synthase (NOS) and that FAD-linked N141I-PS2, another member of the PS family, causes neuronal cell death through NADPH oxidase. In this study, we examined 27 different FAD-linked mutants of PS1, and found that PS1 mutants with mutations in the N-terminal fragment caused NOS inhibitor (NOSI)-sensitive neuronal cell death; in contrast, the PS1 mutants with mutations in the C-terminal fragment caused NOSI-resistant neuronal cell death. The former toxicity was resistant to the specific NADPH oxidase inhibitor apocynin and was inhibited by Humanin (HN), a newly identified neuroprotective factor against Alzheimer's disease (AD)-relevant insults, but not by insulin-like growth factor-I (IGF-I). In contrast, the latter toxicity was sensitive to apocynin and inhibited by both IGF-I and HN. This study indicates for the first time that N- and C-terminal fragment PS1 mutants can generate distinct neurotoxic signals, which will provide an important clue to the understanding of the entire array of neurotoxic signals generated by FAD-causative mutations of PS1.

Key words: Alzheimer's disease; NOS; NADPH oxidase; IGF-I; Humanin

Alzheimer's disease (AD) is the most prevalent neurodegenerative disease associated with progressive dementia. No fundamental therapy for this disease has thus far been developed. In AD, neuronal cell death is the central abnormality that must be controlled by therapeutic agents. Although familial AD (FAD) is caused by mutations in certain genes, such as those for amyloid-β protein precursor (AβPP), presenilin (PS)1, and PS2 (another member of the PS family; see Niikura et al., 2002 for review, it is not well understood how these mutant genes cause neuronal cell death in FAD cases. Multiple studies (Yamatsuji et al., 1996; Wolozin et al., 1996; Guo et al., 1996, 1999a,b; Zhao et al., 1997; Zhang et al., 1998; Czech et al., 1998; Luo et al., 1999; Weihl et al., 1999; Hashimoto et al., 2000a, 2001a–c, 2002a,b), however, have found that expression of all these FAD mutant genes causes or enhances cell death in primary neurons and neuronal cell lines, suggesting that neurotoxicity by FAD genes may play a direct role in the pathogenesis of AD, at least to a certain extent. It is thus important to understand the intracellular death signals generated by FAD mutant genes in cultured neuronal cells.

Recent studies indicate that FAD-linked mutant PS1 enhances cell death in T lymphocytes (Wolozin et al., 1998), PC12 cells (Guo et al., 1996; Weihl et al., 1999), rat primary cultured neurons (Guo et al., 1999a; Zhang et al., 1998; Czech et al., 1998; Weihl et al., 1999), and neurohybrid cells (Hashimoto et al., 2002b). We have shown previously that M146L-PS1, a representative FAD-linked mutant, causes nonapoptotic cell death in F11 neurohybrid cells (Hashimoto et al., 2002b). F11 cells, the hybrid of a rat embryonic primary neuron and a mouse neuroblastoma cell, are one of the best immortalized models for primary cultured neurons as they carry representative characteristics of primary neurons, such as generation of action potentials without differentiation by nerve growth factor (NGF) (Platika et al., 1985). These cells have been used in various studies of neuronal functions

Contract grant sponsor: Keio Gijuku Academic Development Funds (Y.H.) and grants from the Japan Society for the Promotion of Science.

*Correspondence to: Ikuo Nishimoto and Takako Niikura, Department of Pharmacology, KEIO University School of Medicine, General Research Building, 3rd and 6th Floors, 35 Shinanomachi, Tokyo 160-8582, Japan. E-mail: niikurat@sc.itc.keio.ac.jp

Received 11 April 2003; Revised 10 October 2003; Accepted 10 October 2003

(Yamatsuji et al., 1996; Storms and Rutishauser, 1998; Huang et al., 2000; Hagiwara et al., 2000; Ghil et al., 2000; Sudo et al., 2000; Hashimoto et al., 2001a,b,c; Niikura et al., 2001). Using these cells, we showed that FAD-linked M146L-PS1 causes neuronal cell death through nitrogen oxide synthase (NOS) and that FAD-linked N141I-PS2, another PS family, causes neuronal cell death through NADPH oxidase (Hashimoto et al., 2002b). Therefore, two possibilities are conceivable. One possibility is that FAD-linked mutants of PS1 cause NOS-mediated cell death as a function different from that of FAD-linked PS2 mutants. In this case, all FAD-linked mutants of PS1 cause cell death only through NOS. Another possibility is that PS1 has the potential to cause NADPH oxidase-mediated cell death and that some FAD-linked mutants of PS1 can cause cell death through NADPH oxidase, as is the case with mutant PS2.

Although FAD is caused by only a few mutations in PS2, various mutations in PS1 cause FAD. PS proteins consist of N-terminal and C-terminal fragments (NTF and CTF) that are generated by cleavage of PS holoproteins. The FAD-causative mutations could be located in both the NTF and CTF of PS1. The M146L mutation, which turns on the NOS-mediated toxic pathway, is located in the NTF of PS1. The present study was conducted to clarify whether other mutations of PS1 can trigger the NADPH oxidase-mediated toxic pathway or whether PS1 mutants can cause only NOS-mediated cell death. We investigated 27 mutations of PS1, scattered from the N terminus to the C terminus.

MATERIALS AND METHODS

M146L-PS1 cDNA was kindly provided by Dr. P. St.-George Hyslop (Centre for Research in Neurodegenerative Disease, University of Toronto, Toronto, Canada), subcloned to pcDNA, and described in detail in Hashimoto et al. (2002b). Other mutants of PS1 (V82L, V96P, Y115H, E120K, M139T, M139V, M139I, I143F, M146V, H163R, H163Y, I213T, A231T, L250S, A260V, C263R, P264L, P267S, R269H, E280A, E280G, E318G, G384A and L392V) in the pCIneo plasmid have been described previously in Murayama et al. (1999). A246E-PS1 and C410Y-PS1 were subcloned into pIND plasmid (Invitrogen) with sequence confirmation. Ac-DEVD-CHO (acetyl-L-aspartyl-L-glutamyl-L-valyl-L-aspartyl-al, abbreviated DEVD) and Humanin (HN) were from Peptide Institute Inc. (Minoh, Osaka, Japan). Glutathione-ethyl-ester (GEE) and apocynin (4-hydroxy-3 methoxyacetophenone; APO) were purchased from Sigma-Aldrich (Tokyo, Japan). IGF-I was purchased from Roche Diagnostics (Mannheim, Germany). Ponasterone (Invitrogen) was employed as ecdysone (EcD). N^G-monomethyl-D-arginine monoacetate salt(L-NMMA) was from Calbiochem (San Diego, CA).

F11 cells were grown in Ham's F-12 media plus 18% fetal bovine serum (FBS) and antibiotics as described previously (Hashimoto et al., 2001a,b,c). For transient transfection, F11 cells were seeded at 7×10^4 cells/well in a 6-well plate and cultured in Ham's F-12 plus 18% FBS for 12–16 hr. Cells were transfected with pcDNA or pCIneo plasmids (1 μg plasmid, 2 μl LipofectAMINE, 4 μl/well PLUS reagent) in the absence of serum for 3 hr. After subsequent incubation with Ham's F-12 plus 18%FBS for 2 hr, cells were cultured in Ham's F-12 plus 10% FBS. Twenty-four hours after the onset of transfection, cells were cultured in Ham's F-12 plus N2 supplement (Gibco-BRL, Gaitherburg, MD) with or without inhibitors. Cell mortality was measured by Trypan blue exclusion assay at 72 hr after onset of transfection.

F11 cells overexpressing both the EcD receptor (EcR) and the retinoid X receptor (RXR) (F11/EcR cells) have been described previously (Hashimoto et al., 2000a, 2002a,b). For transient transfection of the pIND plasmids, F11/EcR cells were seeded at 7×10^4 cells/well in a 6-well plate and cultured in Ham's F-12 plus 18% FBS for 12–16 hr, and were transfected with EcD-inducible pIND plasmids (1 μg pIND plasmids, 2 μl LipofectAMINE, and 4 μl PLUS reagent [Gibco-BRL]) in the absence of serum for 3 hr. After subsequent incubation with Ham's F-12 plus 18% FBS for 12–16 hr, cells were cultured with or without inhibitors in Ham's F-12 plus 10% FBS for 2 hr, and EcD was then added to the media (without medium change). Cell mortality was measured by Trypan blue exclusion assay at 72 hr after the onset of EcD treatment.

NSC-34 cells were kindly provided by Dr. N.R. Cashman (Centre for Research in Neurodegenerative Diseases and Sunnybrook and Women's College Health Sciences Centre, University of Toronto, Ontario, Canada). Experiments using NSC-34 cells were carried out in the same manner as those using F11 cells.

The Trypan blue exclusion assay has been described previously in detail (Hashimoto et al., 2000a,b). Briefly, at the termination of experiments, cells were suspended by pipetting gently, and 50 μl of 0.4% Trypan blue solution (Sigma-Aldrich Japan) was mixed with 200 μl of the cell suspension (final concentration 0.08%) at room temperature. Stained cells were counted within 3 min after the mixture with Trypan blue solution. Cell mortality was then determined as a percentage of Trypan blue-stained cells in total cells. Cell mortality assessed by this method thus represents the population of dead cells in total cell population, including both adhesive and floating cells, at the termination of experiments.

WST-8 cell viability assay was carried out using Cell Counting Kit-8 (Wako Pure Chemicals, Osaka, Japan), as described previously (Hashimoto et al., 2000b). Seventy-two hours after Aβ treatment, cells were added with 10 μl WST-8 solution. After 2-hr incubation in a CO_2 incubator at 37°C, WST-8 absorbance was measured as optical density $(OD)_{450}$. Most cell viability data using WST-8 assay were obtained from neurons seeded at 5×10^4 cells/well in 96-well plates and confirmed by Trypan blue assay with cells seeded at 2.5×10^4 cells/well. In F11 neurohybrid cells, the data of Trypan blue exclusion assay were reciprocal with the data of WST-8 assay, indicating that Trypan blue exclusion assay is a reliable method to assess cell viability (Hashimoto et al., 2000b).

Immunoblot analysis of expressed constructs was carried out as follows. SDS-PAGE of cell lysates (20 μg/lane) were carried out, and separated proteins were transferred onto polyvinylidene difluoride (PVDF) sheets. After blocking with 10% skim milk in PBST (137 mM NaCl, 2.7 mM KCl, 4.3 mM $Na_2HPO_4 \cdot 7H_2O$, 1.4 mM KH_2PO_4 containing 0.1% Tween

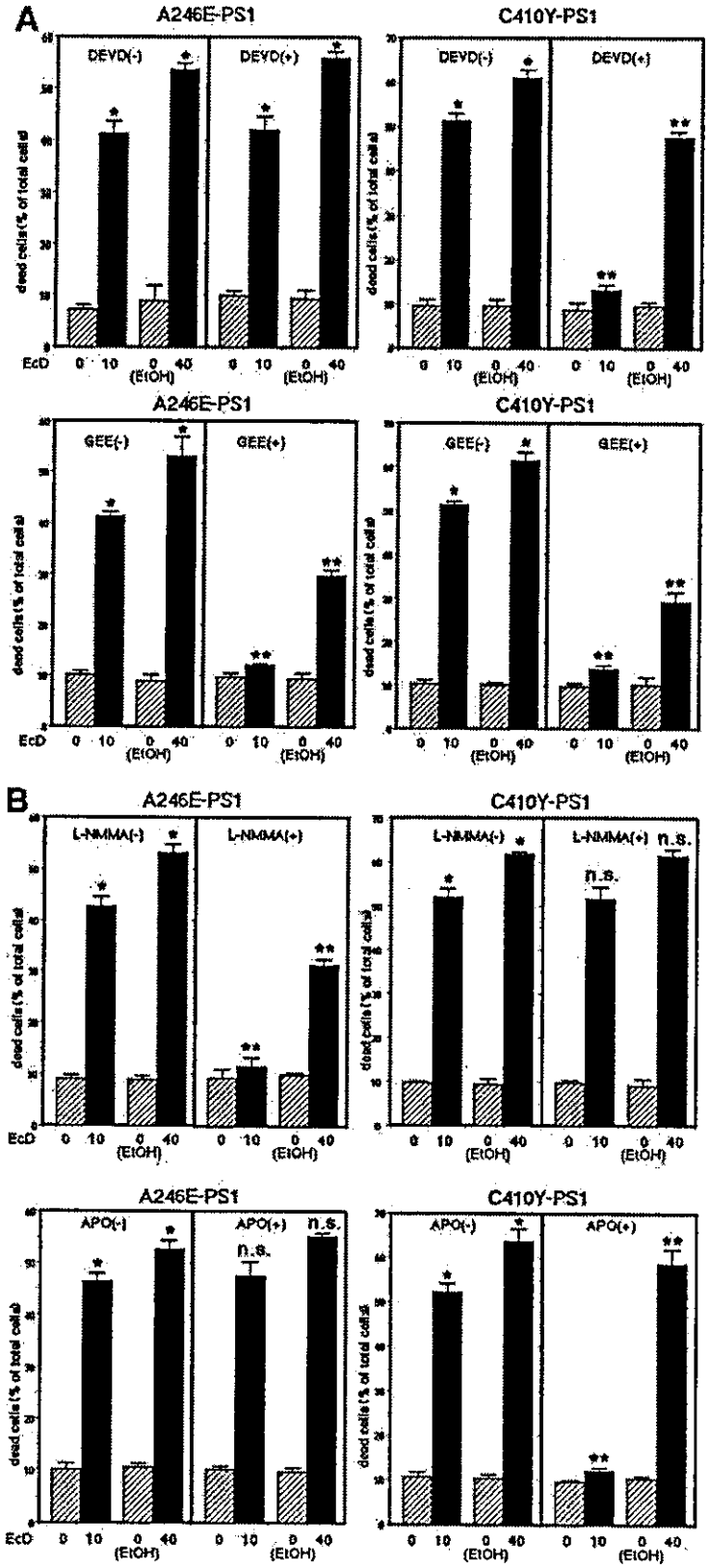

Fig. 1. Effects of various inhibitors on A246E-PS1-induced and C410Y-PS1-induced cell death in F11/EcR cells. A: Effects of DEVD and GEE. F11/EcR cells were transfected with pIND-A246E-PS1 or pIND-C410Y-PS1 and treated with 0, 10, or 40 μM EcD in the absence or presence of 100 μM DEVD or 1 mM GEE. Cell mortality was measured by Trypan blue exclusion assay 72 hr after the onset of EcD treatment. As another negative control, 40 μM EcD-equivalent volume (20 μl) of EtOH, the vehicle of EcD, was used under the same condition (0 EtOH). Values indicate means ± SD of three independent experiments. *Significant vs. corresponding controls without EcD; **significant vs. corresponding controls without inhibitors. B: Effects of L-NMMA and APO. F11/EcR cells were transfected with pIND-A246E-PS1 or pIND-C410Y-PS1 and treated with 0, 10, or 40 μM EcD in the absence or presence of 1 mM L-NMMA or 300 μM APO. Cell mortality was measured by Trypan blue exclusion assay 72 hr after the onset of EcD treatment. As another negative control, 40 μM EcD-equivalent volume (20 μl) of EtOH was used under the same condition (0 EtOH). Values indicate means ± SD of three independent experiments. *Significant vs. corresponding controls without EcD; **significant vs. corresponding controls without inhibitors; n.s., not significant vs. corresponding controls without inhibitors.

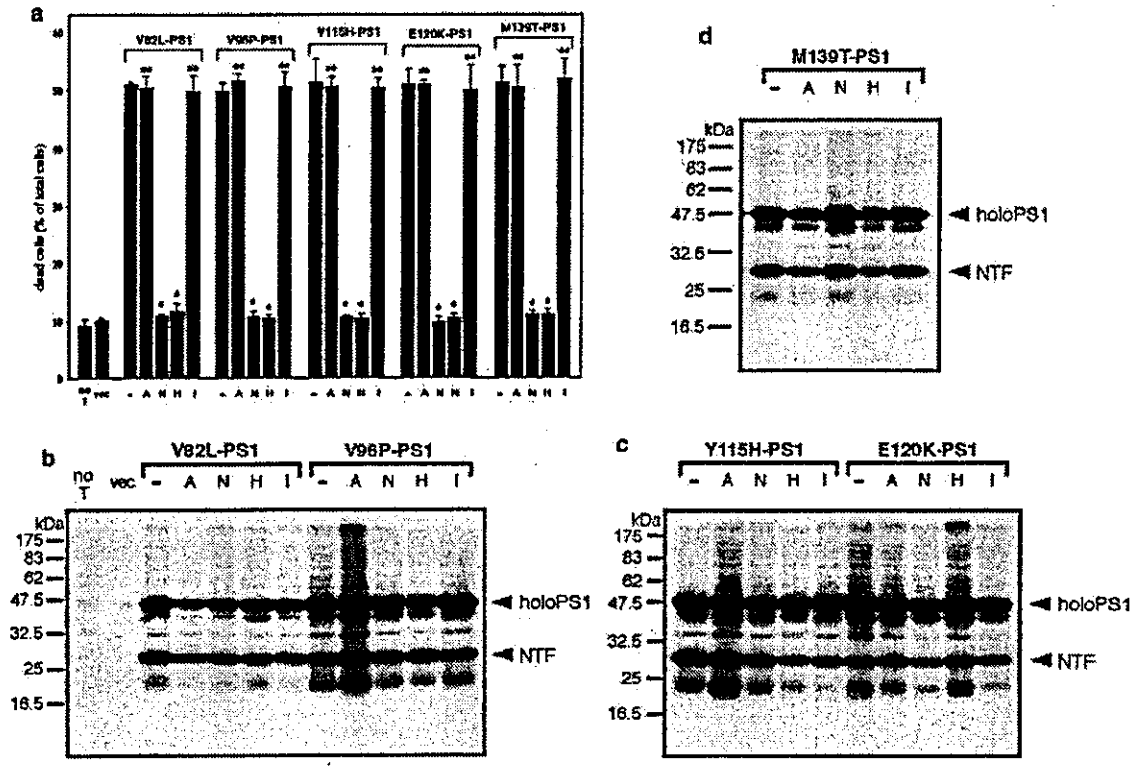

Fig. 2. Inhibitor profiles of cell death by various FAD-linked mutants of PS1. V82L-, V96P-, Y115H-, E120K-, M139T-PS1. F11 cells were transfected with an empty vector (vec), V82L-, V96P-, Y115H-, E120K-, or M139T-PS1 cDNA and cultured in the presence of N2 supplement with or without 300 μM APO (A), 1 mM L-NMMA (N), 10 μM HN (H), or 10 nM IGF-I (I). Seventy-two hours after the onset of transfection, cell mortality was measured by Trypan blue exclusion assay (a). *Significant vs. corresponding controls without inhibitors. **Not significant vs. corresponding controls without inhibitors. Expression of the transfected PS1 mutants was examined by immunoblotting with anti-PS1 antibody (b–d). The upper and lower regions of the two major bands correspond to the holoproteins and the N-terminal fragments of mutant PS1s. no T, no transfection cases; holoPS1, holoprotein of mutant PS1; NTF, NTF of mutant PS1.

20), the blots were probed with the primary antibody, rat anti-PS1 antibody (1:2,000; Chemicon, Temecula, CA), and the secondary antibody (1:2,000, anti-rat IgG conjugated with horseradish peroxidase [HRP]; Wako), followed by visualization of the immunoreactive bands by ECL (Amersham Pharmacia Biotech).

All experiments described in this study were repeated at least three times with independent transfections and treatments, each of which yielded essentially the same result. Statistical analysis was carried with one-way analysis of variance (ANOVA) followed by Scheffe's post-hoc test, in which $P < 0.05$ was assessed as significant.

RESULTS

Characterization of Cell Death by A246E-PS1 and C410Y-PS1 in F11/EcR Neurohybrid Cells

We initially characterized cell death by A246E-PS1 and C410Y-PS1 using F11/EcR cells. These cells are F11 cells stably expressing both EcR and RXR. When F11/EcR cells are transfected with PS1 cDNA (both wild-type and mutant PS1) in pIND (ecdysone responsive plasmid) and treated with EcD, the corresponding PS1 holoproteins are expressed in a manner dependent on the EcD dose.

The pIND-encoded A246E-PS1 and C410Y-PS1 were named pIND-A246E-PS1 and pIND-C410Y-PS1, respectively. When cells were transfected with pIND-A246E-PS1 and treated with 10 μM and 40 μM EcD, cell death was induced in ~40% and ~55% (of total cells), respectively (Fig. 1A, upper left). When cells transfected with pIND-A246E-PS1 were treated with 10 μM and 40 μM EcD in the presence of 100 μM DEVD, cell death was induced at the same extent as that in the absence of DEVD (Fig. 1A, upper left). DEVD is a well-established cell-permeable caspase inhibitor. Similarly, when cells were transfected with pIND-C410Y-PS1 and treated with 10 μM and 40 μM EcD, cell death was induced in ~50% and ~60% (of total cells), respectively (Fig. 1A, upper right). In contrast to A246E-PS1, however, when cells transfected with pIND-C410Y-PS1 were treated with 10 μM and 40 μM EcD in the presence of 100 μM DEVD, cell death was inhibited significantly (Fig. 1A, upper right). These data suggest that C410Y-PS1-induced cell

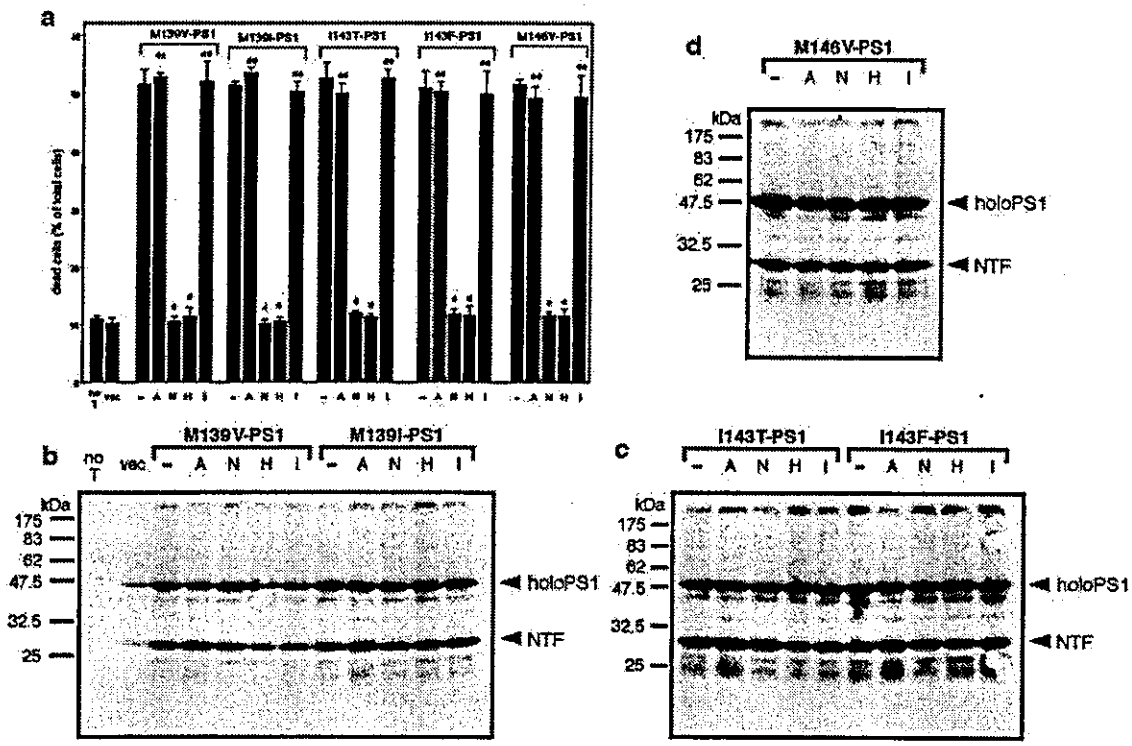

Fig. 3. M139V/I-, I143T/F-, M146V-PS1. F11 cells were transfected with an empty vector (vec), M139V-, M139I-, I143T-, I143F-, or M146V-PS1 cDNA and cultured in the presence of N2 supplement with or without 300 μM APO (A), 1 mM L-NMMA (N), 10 μM HN (H), or 10 nM IGF-I (I). Seventy-two hours after the onset of transfection, cell mortality was measured by Trypan blue exclusion assay (a). Expression of the transfected PS1 mutants was examined by immunoblotting with anti-PS1 antibody (b–d). The upper and lower regions of the two major bands correspond to the holoproteins and the N-terminal fragments of mutant PS1s. no T, no transfection cases; holoPS1, holoprotein of mutant PS1; NTF, NTF of mutant PS1.

death was sensitive to DEVD, whereas A246E-PS1-induced cell death was resistant to DEVD.

Similar experiments were carried out with GEE instead of DEVD. GEE is a well-established cell-permeable antioxidant. When F11/EcR cells transfected with pIND-A246E-PS1 were treated with 10 μM and 40 μM EcD in the presence of 1 mM GEE, cell death was inhibited significantly (Fig. 1A, lower left). This was also the case with C410Y-PS1. Similarly, when cells transfected with pIND-C410Y-PS1 were treated with EcD in the presence of 1 mM GEE, the extent of cell death was inhibited significantly (Fig. 1A, lower right). These data suggest that both A246E-PS1-induced and C410Y-PS1-induced cell deaths were sensitive to GEE.

Our earlier studies showed that M146L-PS1-induced cell death is resistant to DEVD and mediated by NOS, whereas N141I-PS2-induced cell death is sensitive to DEVD and mediated by NADPH oxidase (Hashimoto et al., 2002a,b). We thus examined whether A246E-PS1-induced cell death and C410Y-PS1-induced cell death are sensitive to NOS and NADPH oxidase inhibitors. As shown in Figure 1B, A246E-PS1-induced cell death was sensitive to 1 mM L-NMMA, but not 300 μM APO. Under the same conditions, C410Y-PS1-induced cell death was sensitive to 300 μM APO, but not 1 mM L-NMMA. L-NMMA and APO are specific inhibitors of NOS and NADPH oxidase, respectively, and 1 mM L-NMMA and 300 μM APO selectively inhibit NOS and NADPH oxidase, respectively. These data suggest that A246E-PS1-induced cell death is most likely mediated by NOS, but not NADPH oxidase, whereas C410Y-PS1-induced cell death is most likely mediated by NADPH oxidase, but not by NOS.

Taken together, these data indicate that A246E-PS1 induces cell death by triggering the same NOS-mediated DEVD-resistant pathway triggered by M146L-PS1 and that C410Y-PS1 induces cell death by triggering a different NADPH oxidase-mediated DEVD-sensitive pathway.

Sensitivities of FAD-Linked Mutant PS1-Induced Cell Death to NOS and NADPH Oxidase Inhibitors in F11 Neurohybrid Cells

Based on these results, we next investigated the relationship between the location of FAD mutations in PS1 and types of induced cell death. For this purpose, we used a simple F11 cell system in which F11 cells were

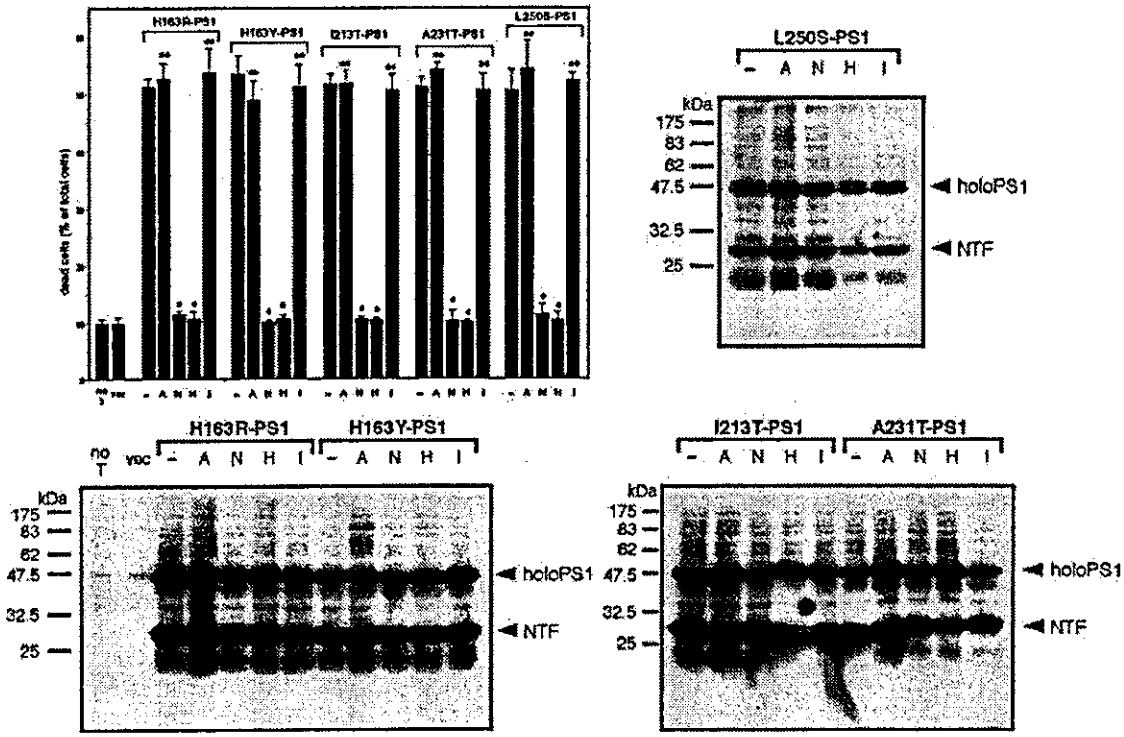

Fig. 4. H163R/Y-, I213T-, A231T-, L250S-PS1. F11 cells were transfected with an empty vector (vec), H163R-, H163Y-, I213T-, A231T-, or L250S-PS1 cDNA and cultured in the presence of N2 supplement with or without 300 μM APO (A), 1 mM L-NMMA (N), 10 μM HN (H), or 10 nM IGF-I (I). Seventy-two hours after the onset of transfection, cell mortality was measured by Trypan blue exclusion assay (a). *Significant vs. corresponding controls without inhibitors. **Not significant vs. corresponding controls without inhibitors. Expression of the transfected PS1 mutants was examined by immunoblotting with anti-PS1 antibody (b–d). The upper and lower regions of the two major bands correspond to the holoproteins and the N-terminal fragments of mutant PS1s. no T, no transfection cases; holoPS1, holoprotein of mutant PS1; NTF, NTF of mutant PS1.

transfected with mutant PS1 cDNA and cultured in the presence of N2 supplement. Under the condition of the F11 cell system, M146L-PS1-induced cell death is mechanistically the same as M146L-PS1-induced cell death under the condition of F11/EcR cell system with 10 μM EcD (data not shown). We therefore transfected F11 cells with various PS1 mutant cDNAs and cultured cells with L-NMMA or APO in the presence of N2 supplement.

V82L, V96P, Y115H, E120K, and M139T. As shown in Figure 2, cell deaths induced by V82L-, V96P-, Y115H-, E120K-, and M139T-PS1 were inhibited by 1 mM L-NMMA, but resistant to 300 μM APO. Expression of V82L-, V96P-, Y115H-, E120K-, or M139T-PS1 was not inhibited by 1 mM L-NMMA and 300 μM APO (Fig. 2). As compared to the internal control actin, the expression levels of these PS1 mutants were thought to be equivalent, even when APO or other inhibitors were treated (data not shown). These results suggest that V82L-, V96P-, Y115H-, E120K-, and M139T-PS1 induce cell death by triggering the same pathway as M146L-PS1 triggers.

M139V, M139I, I143T, I143F, and M146V. As shown in Figure 3, cell deaths induced by M139V-, M139I-, I143T-, I143F-, and M146V-PS1 were inhibited by 1 mM L-NMMA, but resistant to 300 μM APO. Expression of M139V-, M139I-, I143T-, I143F-, or M146V-PS1 was not inhibited by 1 mM L-NMMA and 300 μM APO (Fig. 3). As compared to the internal control actin, the expression levels of these PS1 mutants were thought to be equivalent, even when APO or other inhibitors were treated (data not shown). These results suggest that M139V-, M139I-, I143T-, I143F-, and M146V-PS1 induce cell death by triggering the same pathway as M146L-PS1 triggers.

H163R, H163Y, I213T, A231T, and L250S. As shown in Figure 4, cell deaths induced by H163R-, H163Y-, I213T-, A231T-, and L250S-PS1 were inhibited by 1 mM L-NMMA, but resistant to 300 μM APO. Expression of H163R-, H163Y-, I213T-, A231T-, or L250S-PS1 was not inhibited by 1 mM L-NMMA and 300 μM APO (Fig. 4). As compared to the internal control actin, the expression levels of these PS1 mutants were thought to be equivalent, even when treated with APO or other inhibitors (data not shown). These results suggest that H163R-, H163Y-, I213T-, A231T-, and